

# SUPPORTING INFORMATION

## **Understanding the optical properties of doped and undoped 9-armchair graphene nanoribbons in dispersion**

*Sebastian Lindenthal<sup>1</sup>, Daniele Fazzi<sup>2</sup>, Nicolas F. Zorn<sup>1</sup>, Abdurrahman Ali El Yumin<sup>1</sup>, Simon Settele<sup>1</sup>, Britta Weidinger<sup>3</sup>, Eva Blasco<sup>3</sup>, Jana Zaumseil<sup>\*1</sup>*

<sup>1</sup>Institute for Physical Chemistry, Heidelberg University, D-69120 Heidelberg, Germany  
E-mail: zaumseil@uni-heidelberg.de

<sup>2</sup> University of Bologna, Department of Chemistry, 40126, Bologna, Italy

<sup>3</sup> Institute for Molecular Systems Engineering and Advanced Materials and Institute of Organic Chemistry, Heidelberg University, D-69120 Heidelberg, Germany

\*E-mail: zaumseil@uni-heidelberg.de

## Contents

|  |      |
|--|------|
| Synthesis of 9-aGNRs .....                                       | S-3  |
| NMR spectra.....   | S-12 |
| Supporting Figures – Spectroscopic Characterization 9-aGNRs..... | S-18 |
| Quantum chemical calculations of neutral 9-aGNRs.....            | S-29 |
| Supporting Figures – Doped 9-aGNRs .....                         | S-34 |
| Quantum chemical calculations of charged 9-aGNRs .....           | S-35 |
| REFERENCES .....   | S-36 |

## Synthesis of 9-aGNRs

### General

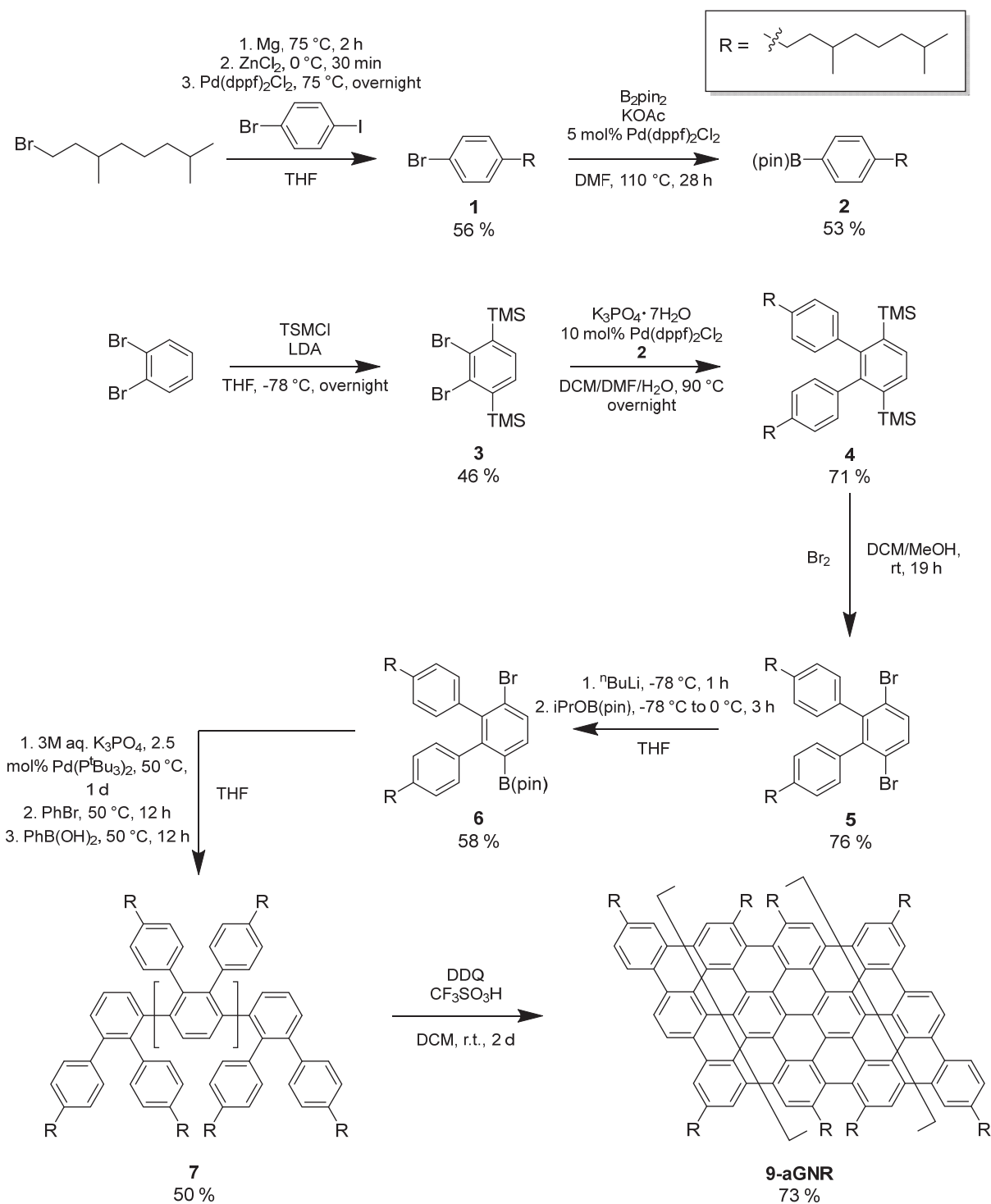
The synthesis of 9-aGNRs follows the published method by Li *et al.*<sup>1</sup> with some minor modifications.

Reagent grade chemicals were purchased from Sigma Aldrich, Alfa Aesar, Tokio Chemical Industries or Fisher Scientific and used without further purification. Anhydrous solvents were obtained from an MBraun MB SPS-800 solvent purification system, with the exception of dry THF, which was freshly distilled over sodium prior to usage. All reactions containing moisture or air-sensitive components were carried out in inert atmosphere and in dry reaction vessels with standard Schlenk techniques unless noted otherwise.

For analytical thin-layer chromatography (TLC) aluminum plates coated with 0.2 mm of silica gel and fluorescent indicator (Macherey-Nagel, ALUGRAM®, SIL G/UV<sub>254</sub>) were used. Spots on TLC plates were observed by exposure to UV light ( $\lambda = 254$  nm and 366 nm). Column chromatography was performed on silica gel (Macherey-Nagel, M-N Silica Gel 60A, 230-400 mesh).

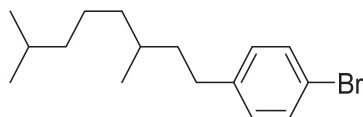
<sup>1</sup>H and <sup>13</sup>C NMR spectra were recorded either on a Bruker Avance DRX 300 (300 MHz for <sup>1</sup>H and 75 MHz for <sup>13</sup>C), Bruker Avance III 400 (400 MHz for <sup>1</sup>H and 100 MHz for <sup>13</sup>C) or Bruker Avance III 600 (600 MHz for <sup>1</sup>H and 150 MHz for <sup>13</sup>C) spectrometer. Chemical shifts  $\delta$  are reported in ppm and referenced to the residual solvent signal ( $\delta_{\text{H}}(\text{CHCl}_3) = 7.26$  ppm,  $\delta_{\text{C}}(\text{CHCl}_3) = 77.2$  ppm). Coupling constants (J) are given in Hz. To report the multiplicity the following abbreviations were used: s = singlet, d = doublet and m = multiplet for the <sup>1</sup>H NMR and s = primary, d = secondary, t = tertiary and q = quarternary for <sup>13</sup>C NMR.

GPC measurements were performed on a Shimadzu Nexera LC-40 system (with LC-40D pump, autosampler SIL-40C, DGU-403 (degasser), CBM-40 (controlling unit), column oven CTO-40C, UV-detector SPD40 and RI-detector RID-20A). The system was equipped with 4 analytical GPC-columns (PSS): 1 x SDV precolumn 3  $\mu\text{m}$  8x50 mm, 2 x SDV column 3  $\mu\text{m}$  1000Å 8x300 mm, 1 x SDV column 3  $\mu\text{m}$  10<sup>4</sup>Å 8x300 mm. The measurements were performed in THF at a flow speed of 1 mL/min at a temperature of 40 °C. Chromatograms were analyzed using the LabSolutions (Shimadzu) software. Calibration was performed against different or polystyrene standards (370 - 2 520 000 Da, PSS).



**Scheme S1. Synthesis of the 9-aGNR according to Li *et al.*<sup>1</sup>** Reaction conditions were kept constant. Yields of each reaction step are denoted under the respective molecule.

### 1-bromo-4-(3,7-dimethyloctyl)benzene (1)

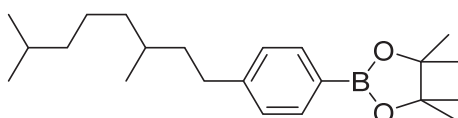


Magnesium shavings (1.47 g, 63.6 mmol) were added to a solution of 1-bromo-3,7-dimethyloctane (4.81 g, 21.7 mmol) in 10 mL dry, degassed THF and stirred at 70 °C for 2 h. The Grignard reagent was slowly added to a solution of dried ZnCl<sub>2</sub> (2.89 g, 21.2 mmol) in 20 mL of dry, degassed THF at 0 °C and stirred for 30 min. After addition of 1-bromo-4-iodobenzene (5.00 g, 17.7 mmol) and Pd(dppf)Cl<sub>2</sub> (388 mg, 0.53 mmol) the reaction mixture was heated to reflux overnight. When heating up the reaction mixture, addition of more THF was necessary as the reaction mixture used to solidify in the reaction vessel. After cooling to room temperature, 50 mL of diethyl ether and 50 mL of 1 M HCl were added to the reaction mixture. The organic phase was separated and the aqueous phase was extracted with 3 x 100 mL of diethyl ether. The combined organic phases were washed with brine and water, dried over Na<sub>2</sub>SO<sub>4</sub> and the solvent was removed by rotary evaporation. The crude product was purified by flash column chromatography (R<sub>f</sub> = 0.9, pure petroleum ether (PE)) to yield **1** as a colorless oil (3.11 g, 59 %).

<sup>1</sup>H NMR (CDCl<sub>3</sub>, 300 MHz): δ 7.38 (m, 2H, Ar-H), 7.05 (m, 2H, Ar-H), 2.65-2.46 (m, 2H), 1.66-1.06 (m, 10H), 0.91 (d, J = 6 Hz, 3H, CH<sub>3</sub>), 0.86 (d, J = 7 Hz, 6H, CH<sub>3</sub>) ppm.

<sup>13</sup>C NMR (CDCl<sub>3</sub>, 300 MHz): δ 142.32, 131.46, 130.31, 119.38, 39.49, 38.99, 37.29, 33.09, 32.59, 28.15, 24.86, 22.89, 22.80, 19.75 ppm.

### 2-(4-(3,7-dimethyloctyl)phenyl)-4,4,5,5-tetramethyl-1,3,2-dioxaborolane (2)

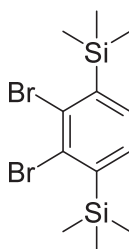


1-bromo-4-(3,7-dimethyloctyl)benzene (5.00 g, 16.8 mmol), 4,4,4',4',5,5,5',5'-octamethyl-2,2'-bi-(1,3,2-dioxaborolane) (4.70 g, 18.5 mmol), potassium acetate (4.95 g, 50.5 mmol) and

Pd(dppf)<sub>2</sub>Cl<sub>2</sub> complex with DCM (dichloromethane, 687 mg, 0.84 mmol) were added to 35 mL of degassed, dry DMF and stirred at 110 °C for 28 h. After cooling down to room temperature 100 mL water and 100 mL ethyl acetate were added to the reaction mixture. The organic phase was separated and the aqueous phase was extracted with 3 x 100 mL of diethyl ether. The combined organic phases were washed with brine and water, dried over Na<sub>2</sub>SO<sub>4</sub> and the solvent was removed under reduced pressure. The crude product was purified by flash column chromatography (R<sub>f</sub> = 0.4, DCM:PE 1:4) to yield **2** as a yellow oil (3.24 g, 56 %).

<sup>1</sup>H NMR (CDCl<sub>3</sub>, 300 MHz): δ 7.72 (m, 2H, Ar-H), 7.20 (m, 2H, Ar-H), 2.72-2.50 (m, 2H), 1.70-1.04 (m, 10H), 1.34 (s, 12H, CH<sub>3</sub>) 0.91 (d, J = 6 Hz, 3H, CH<sub>3</sub>), 0.86 (d, J = 7 Hz, 6H, CH<sub>3</sub>) ppm.

### (2,3-dibromo-1,4-phenylene)bis(trimethylsilane) (**3**)

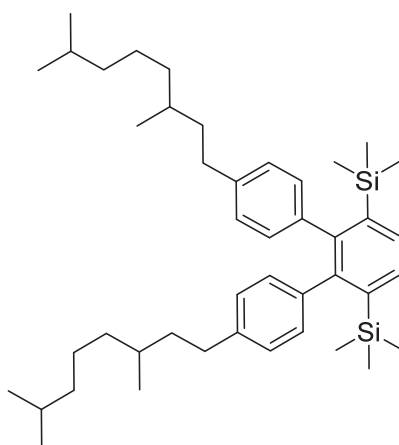


A mixture of dry, degassed THF (3.77 mL, 46.5 mmol), hexane (12.14 mL, 93.0 mmol) and toluene (4.92 mL, 46.5 mmol) was slowly added to solid lithium diisopropylamide (4.98 g, 46.5 mmol) at -78 °C. The slightly yellow LDA solution was then added dropwise to a solution of 1,2-dibromobenzene (5.00 g, 19.7 mmol) and trimethylsilylchloride (5.05 g, 46.5 mmol) at -78 °C. The reaction was stirred at -78 °C overnight. The reaction mixture was then hydrolysed with 50 mL of 0.1M H<sub>2</sub>SO<sub>4</sub>. The yellow organic phase was separated and the aqueous phase was extracted with 3 x 100 mL of diethyl ether. The combined organic phases were washed with brine and water, dried over Na<sub>2</sub>SO<sub>4</sub> and the solvent was removed under reduced pressure. The crude product was purified by flash column chromatography (R<sub>f</sub> = 0.95, pure PE) and recrystallized from a 1:1 mixture of acetone and methanol to yield **3** as colorless crystals (3.43 g, 46 %).

<sup>1</sup>H NMR (CDCl<sub>3</sub>, 600 MHz): δ 7.33 (s, 2H, Ar-H), 0.39 (s, 18H, CH<sub>3</sub>) ppm.

<sup>13</sup>C NMR (CDCl<sub>3</sub>, 150 MHz): δ 145.93, 134.10, 133.52, -0.24 ppm.

**(4,4''-bis(3,7-dimethyloctyl)-[1,1':2',1''-terphenyl]-3',6'-diyl)bis(trimethylsilane) (4)**

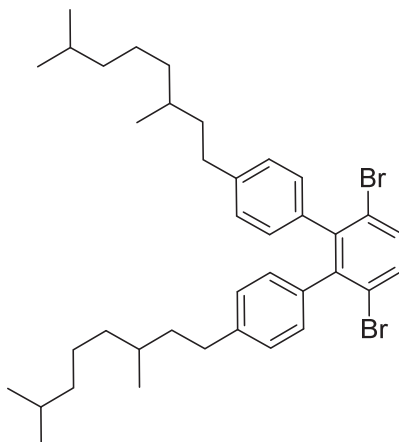


**2** (5.16 g, 15.0 mmol), **3** (1.90 g, 5.00 mmol), Pd(dppf)<sub>2</sub>Cl<sub>2</sub> complex with DCM (408 mg, 0.50 mmol) and K<sub>3</sub>PO<sub>4</sub> · 7 H<sub>2</sub>O (6.36 g, 30.0 mmol) were dissolved in a mixture of 15 mL degassed DMF and 4 mL of degassed H<sub>2</sub>O. The reaction mixture was stirred at 90 °C overnight. After cooling down to room temperature, 100 mL of ethyl acetate and 50 mL of water were added. The organic phase was separated and the aqueous phase was extracted with 3 x 100 mL of diethyl ether. The combined organic phases were washed with brine and water, dried over Na<sub>2</sub>SO<sub>4</sub> and the solvent was removed by rotary evaporation. The crude product was purified by flash column chromatography (R<sub>f</sub> = 0.65, pure PE) to yield **4** as a slightly yellow oil (2.30 g, 69 %).

<sup>1</sup>H NMR (CDCl<sub>3</sub>, 400 MHz): δ 7.61 (s, 2H, Ar-H), 6.87-6.81 (m, 8H, Ar-H), 2.55-2.41 (m, 4H, CH<sub>2</sub>), 1.56-1.06 (m, 20H, CH and CH<sub>2</sub>), 0.88-0.85 (m, 18H, CH<sub>3</sub>), -0.07 (s, 18H, CH<sub>3</sub>) ppm.

<sup>13</sup>C NMR (CDCl<sub>3</sub>, 100 MHz): δ 147.74, 140.91, 140.29, 139.80, 132.66, 131.01, 130.98, 126.86, 126.82, 39.54, 39.06, 37.33, 33.20, 32.29, 28.16, 24.93, 22.90, 22.82, 19.78, 0.66 ppm.

**3',6'-dibromo-4,4''-bis(3,7-dimethyloctyl)-1,1':2',1''-terphenyl (5)**



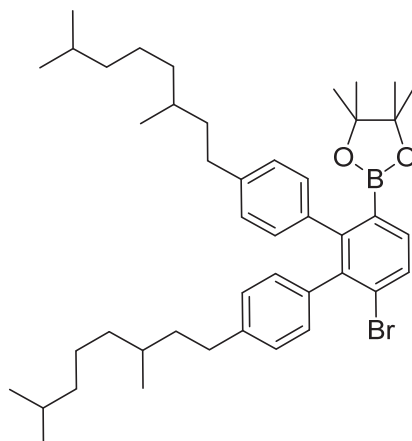
A solution of bromine (1.43 g, 0.46 mL, 8.94 mmol) in 2 mL of DCM was slowly added to a solution of **4** (1.70 g, 2.56 mmol) in 3 mL of dry, degassed DCM and 5 mL of MeOH, which was held at 0 °C. The mixture was then stirred at room temperature overnight. After addition of 50 mL aqueous sodium sulphite solution and 50 mL of DCM, the organic phase was separated and the aqueous phase was extracted with 3 x 100 mL DCM. The combined organic phases were washed with brine and water, dried over Na<sub>2</sub>SO<sub>4</sub> and the solvent was removed by rotary evaporation. The crude product was purified by flash column chromatography ( $R_f = 0.35$ , pure PE) to yield **5** as a yellow oil (1.33 g, 78 %).

<sup>1</sup>H NMR (CDCl<sub>3</sub>, 400 MHz):  $\delta$  7.51 (s, 2H, Ar-H), 6.96-6.93 (m, 4H, Ar-H), 6.86-6.82 (m, 4H, Ar-H), 2.57-2.42 (m, 4H, CH<sub>2</sub>), 1.58-1.06 (m, 20H, CH and CH<sub>2</sub>), 0.88-0.86 (m, 18H, CH<sub>3</sub>) ppm.

<sup>13</sup>C NMR (CDCl<sub>3</sub>, 100 MHz):  $\delta$  144.39, 142.02, 137.53, 132.71, 129.90, 129.88, 127.53, 123.60, 39.54, 38.76, 37.32, 33.32, 32.58, 28.17, 24.90, 22.91, 22.83, 19.83 ppm.



**2-(6'-bromo-4,4''-bis(3,7-dimethyloctyl)-[1,1':2',1''-terphenyl]-3'-yl)-4,4,5,5-tetramethyl-1,3,2-dioxaborolane (6)**

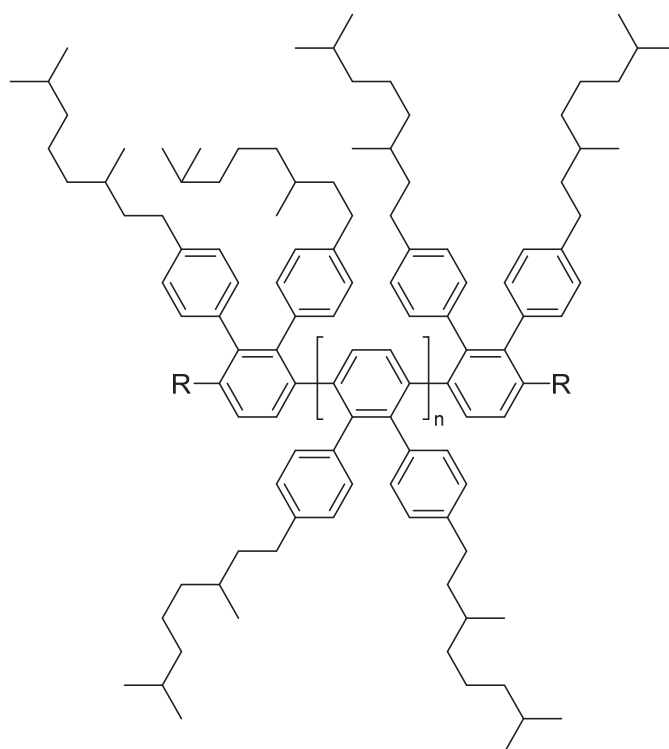


A 2.5 M n-Butyllithium solution in hexane (0.89 mL, 2.22 mmol) was added dropwise to a solution of **5** (1.35 g, 2.02 mmol) in 7 mL dry, degassed THF at -78 °C. The yellow reaction mixture was stirred at -78 °C for 1 h after which 2-isopropoxy-4,4,5,5-tetramethyl-1,3,2-dioxaborolane (0.52 g, 0.57 mL, 2.80 mmol) was added. The white reaction mixture was then stirred for 3 h, during which it was allowed to warm up to 0 °C. After this 50 mL of water and 50 mL of ethyl acetate were added. The organic phase was separated and the aqueous phase was extracted with 3 x 100 mL DCM. The combined organic phases were washed with brine and water, dried over Na<sub>2</sub>SO<sub>4</sub> and the solvent was removed by rotary evaporation. The crude product was purified by flash column chromatography (R<sub>f</sub> = 0.3, 1:4 DCM:PE) to yield **5** as colorless oil (0.83 g, 57 %).

<sup>1</sup>H NMR (CDCl<sub>3</sub>, 400 MHz): δ 7.64 (d, J = 8 Hz, 1H, Ar-H), 7.44 (d, J = 8 Hz, 1H, Ar-H) 6.99-6.81 (m, 8H, Ar-H), 2.64-2.43 (m, 4H, CH<sub>2</sub>), 1.61-1.09 (m, 20H, CH and CH<sub>2</sub>), 1.08 (s, 12H, CH<sub>3</sub>), 0.91-0.81 (m, 18H, CH<sub>3</sub>) ppm.

<sup>13</sup>C NMR (CDCl<sub>3</sub>, 100 MHz): δ 148.57, 141.74, 141.54, 141.15, 139.17, 137.70, 133.60, 131.02, 130.37, 130.33, 130.13, 127.45, 127.10, 126.81, 83.87, 39.58, 39.55, 39.30, 38.74, 37.35, 33.34, 33.24, 32.55, 32.42, 28.16, 24.91, 24.89, 24.68, 22.91, 22.89, 22.83, 22.79, 19.84, 19.73 ppm.

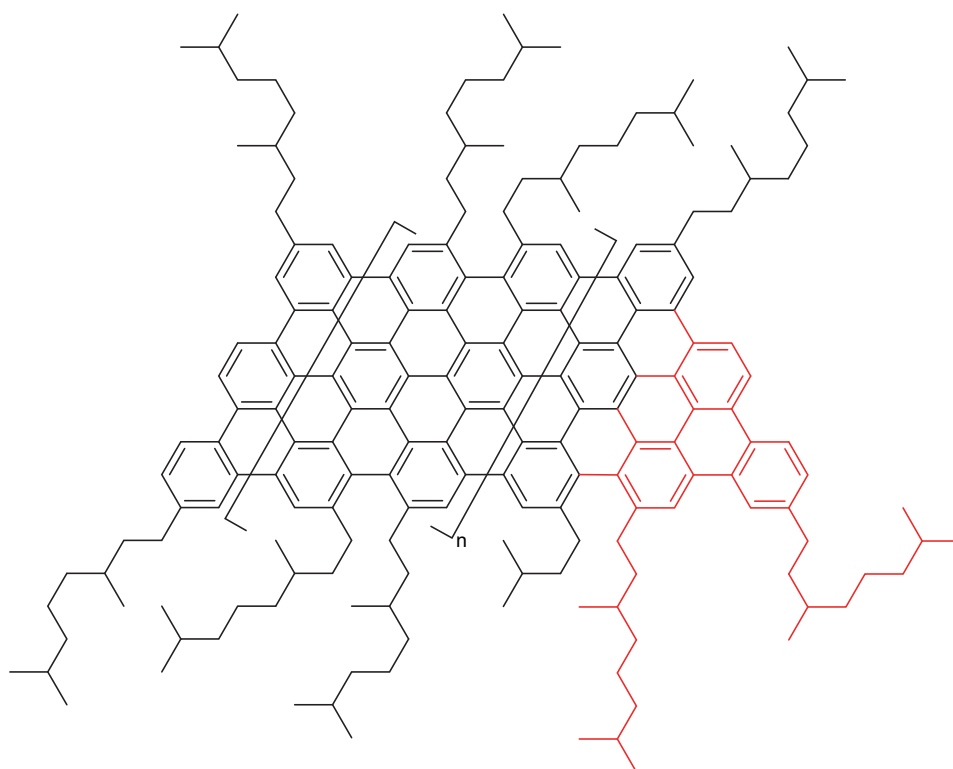
## Synthesis of precursor polymer (7)



Inside of a nitrogen glovebox, the AB-type monomer **6** (102 mg, 0.14 mmol) and  $\text{Pd}(\text{P}^t\text{Bu}_3)_2$  (4 mg, 2.5 mol%) were combined in a Schlenk flask. Under inert atmosphere, 3 mL of degassed THF and 0.7 mL of a 3M  $\text{K}_3\text{PO}_4$  solution in degassed water were added to the reaction mixture. The mixture was stirred at 50 °C for 24h. After that, bromobenzene (21 mg, 0.14 mmol) was added and the reaction was stirred at 50 °C for 8 h. Finally, phenylboronic acid (17 mg, 0.14 mmol) was added and the reaction was stirred at 50 °C for another 8 h. After cooling down to room temperature 10 mL of water and 10 mL of DCM were added to the reaction mixture. The organic phase was separated and the aqueous phase was extracted with 3 x 10 mL DCM. The volume of the combined organic phases was reduced to ~2 mL under reduced pressure and the resulting solution was added to 20 mL of MeOH at room temperature. During this process the polymer precipitates as a white solid. After stirring at room temperature for 1 h, the polymer was filtered and dried under vacuum overnight. To remove impurities and smaller polymer strands, the crude polymer was washed by Soxhlet extraction with acetone for 2 days.

Note that the chemical nature of the end groups R was not determined here. According to Li *et al.* the synthesis usually results in H/H and sometimes H/Phenyl end groups.<sup>1</sup>

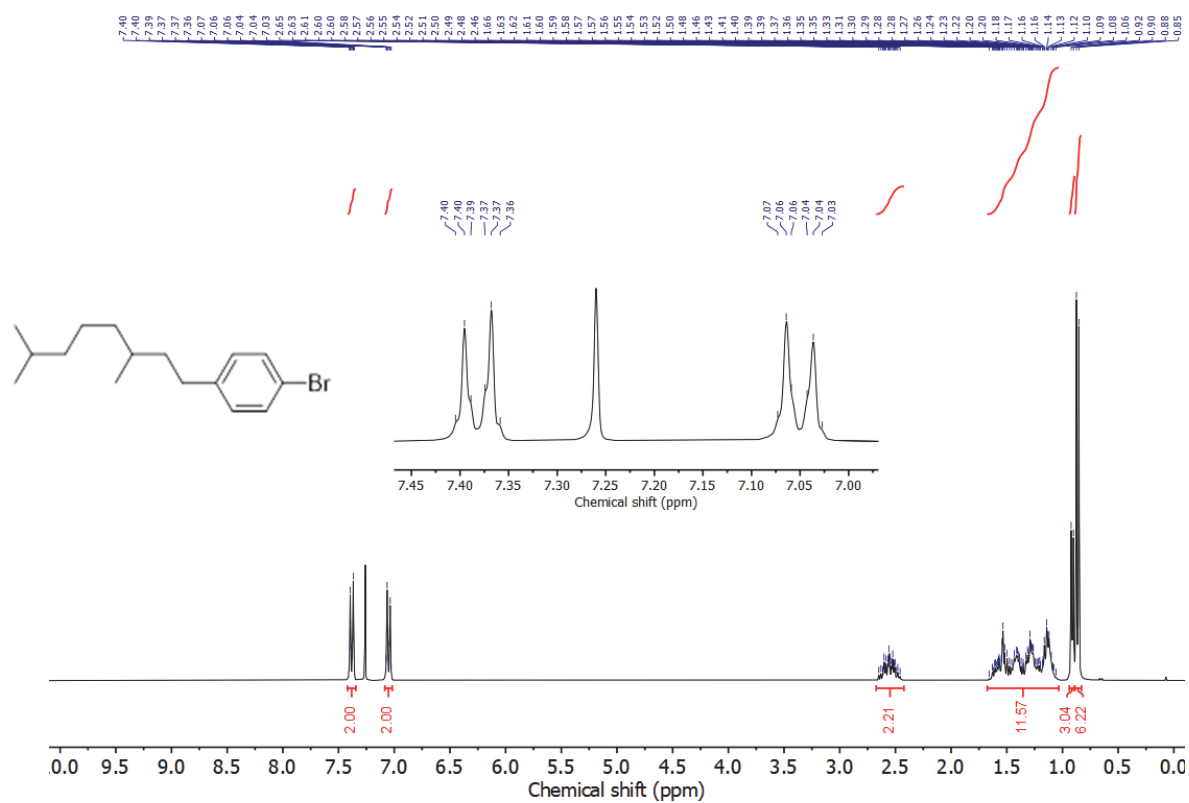
## Synthesis of 9-aGNR



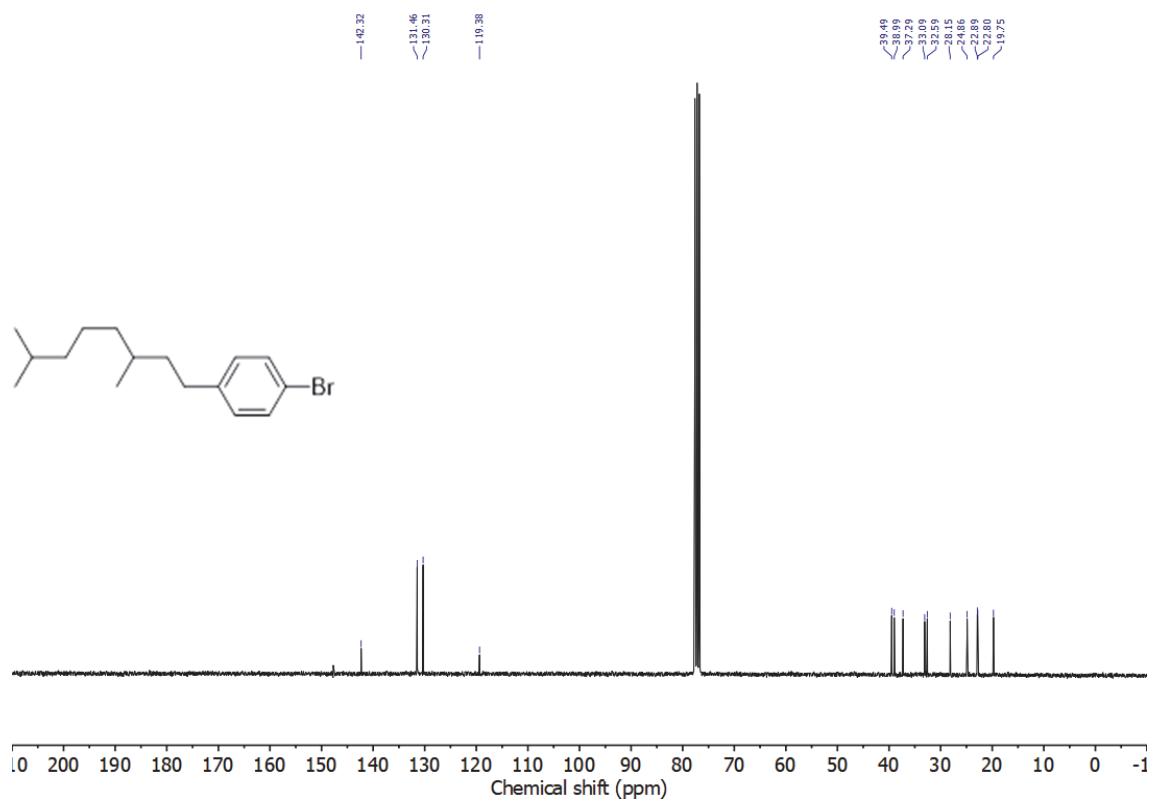
Precursor polymer **7** (202 mg) and DDQ (459 mg) were dissolved in dry, degassed DCM. Dropwise addition of triflic acid (8.6 mL) at 0 °C led to a color change of the reaction mixture from yellow to black. The reaction mixture was stirred at room temperature for 2 days. Subsequently, the reaction mixture was quenched with saturated NaHCO<sub>3</sub> solution until no more CO<sub>2</sub> emerged upon addition (after ~30 mL). The black precipitate was filtered off and washed thoroughly with 200 mL of water, methanol and acetone each. The crude product was then purified by Soxhlet extraction with acetone for 2 days.

Note that depending on the number of terphenyl units in the precursor polymer, the resulting 9-aGNR can either have a parallel shape (black structure, even number of terphenyl units) or a trapezoidal shape (black + red structure, odd number of terphenyl units).

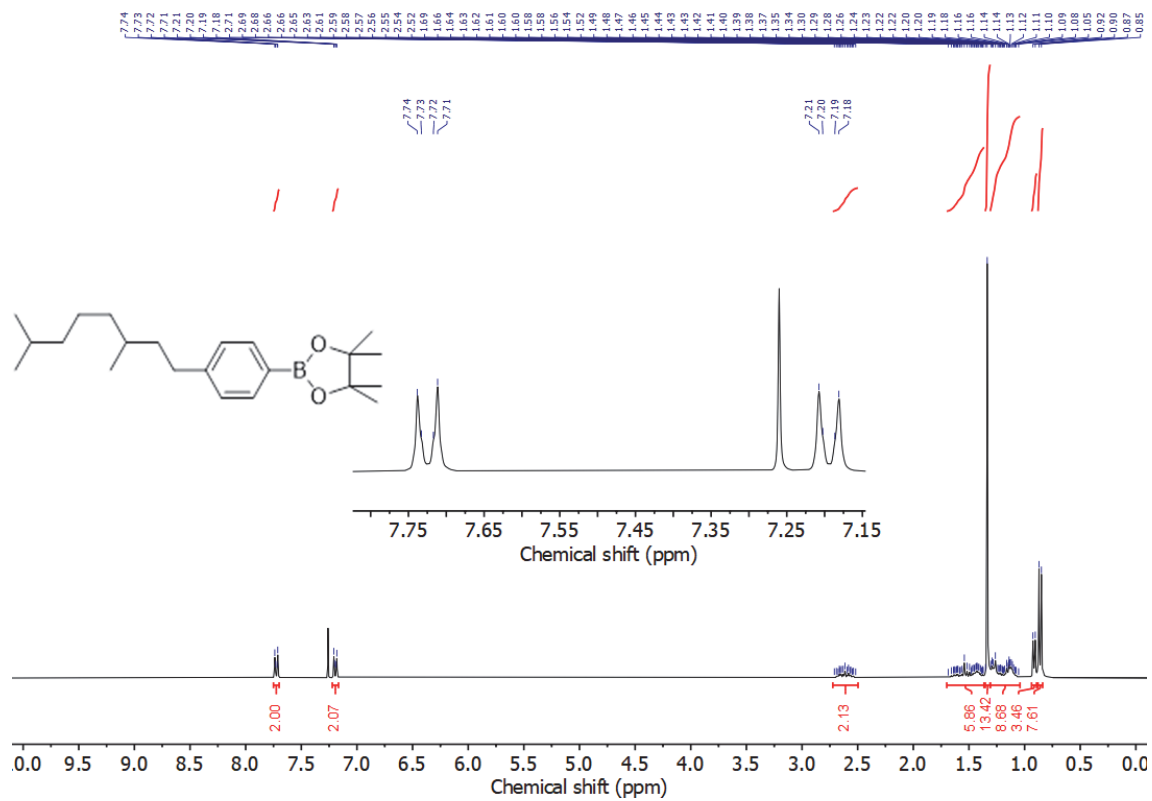
# NMR spectra



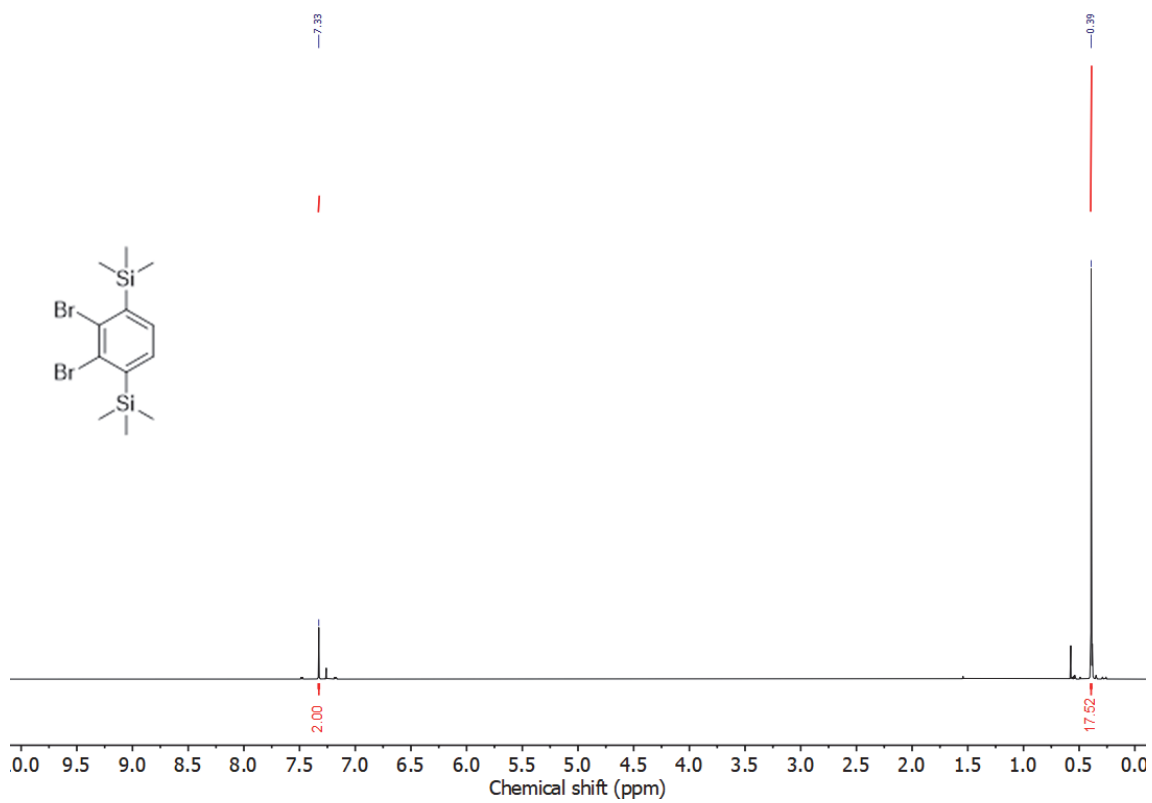
<sup>1</sup>H NMR spectrum of 1 (CDCl<sub>3</sub>, 300 MHz, 25°C)



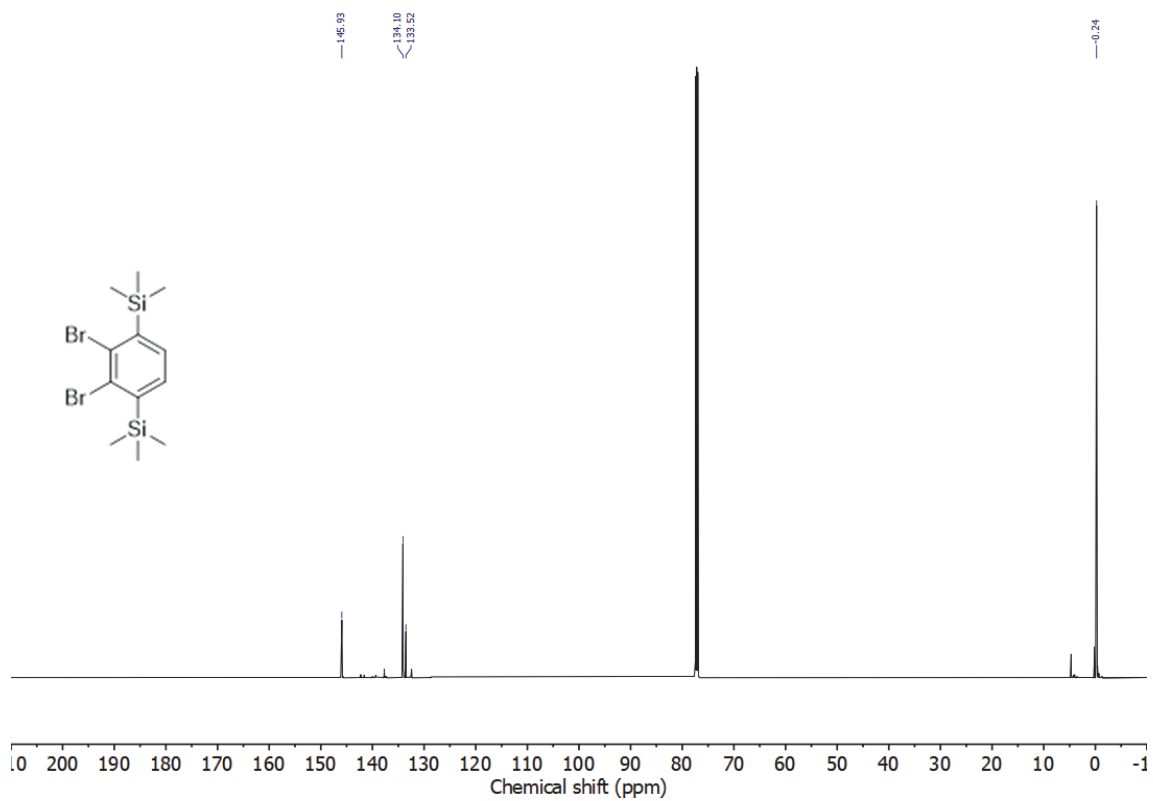
<sup>13</sup>C NMR spectrum of 1 (CDCl<sub>3</sub>, 75 MHz, 25°C)



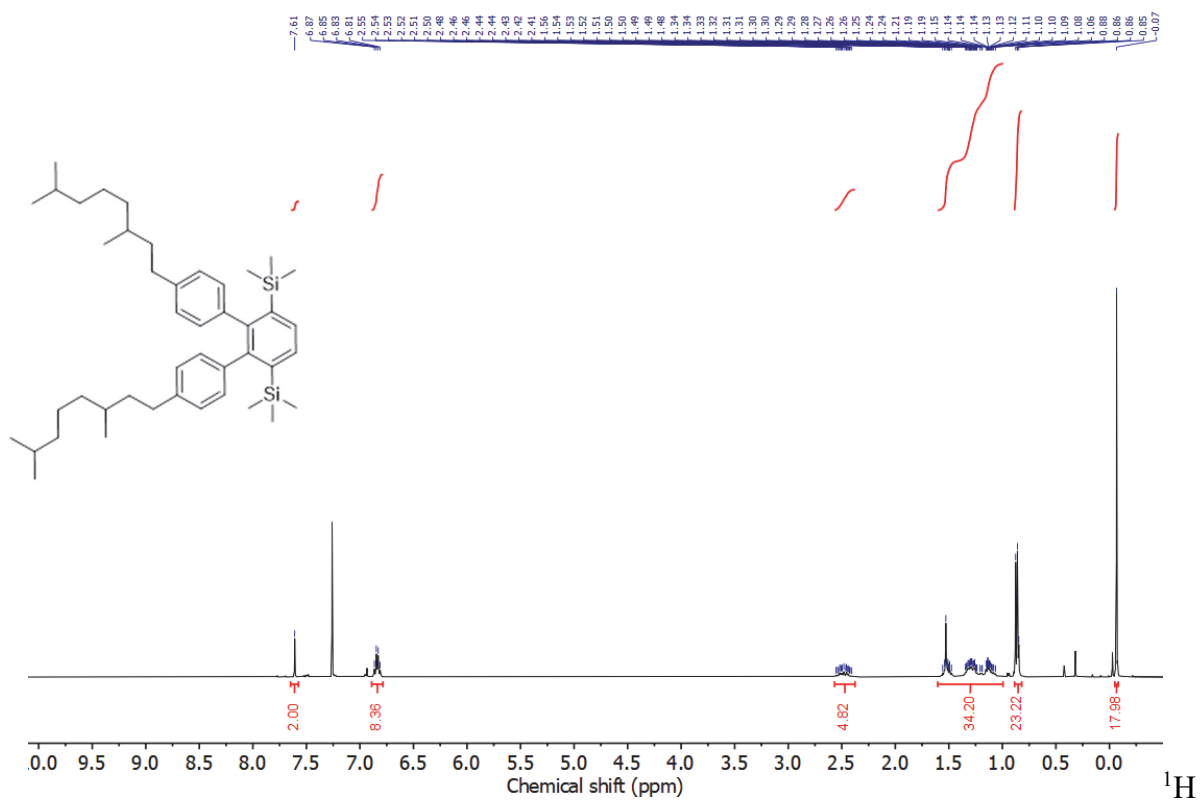
$^1\text{H}$  NMR spectrum of **2** ( $\text{CDCl}_3$ , 300 MHz,  $25^\circ\text{C}$ )



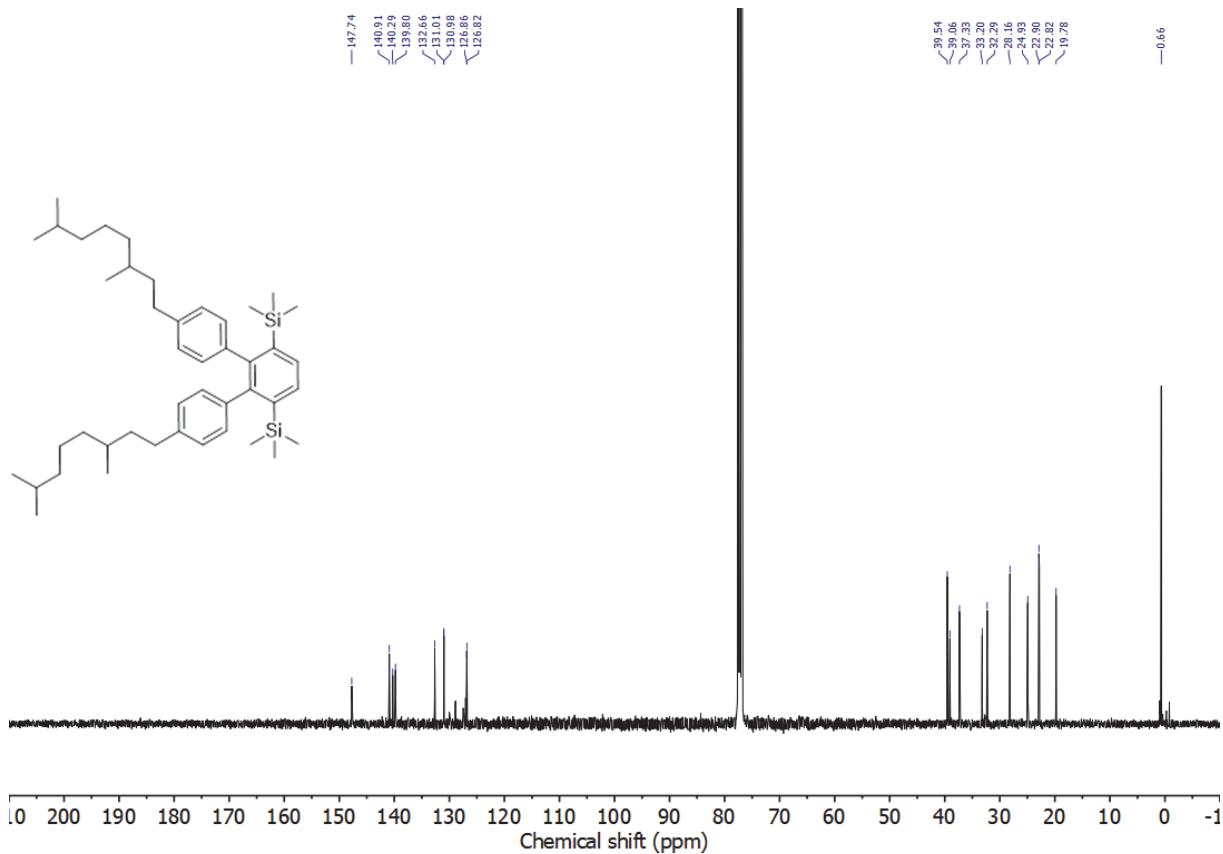
$^1\text{H}$  NMR spectrum of **3** ( $\text{CDCl}_3$ , 600 MHz,  $25^\circ\text{C}$ )



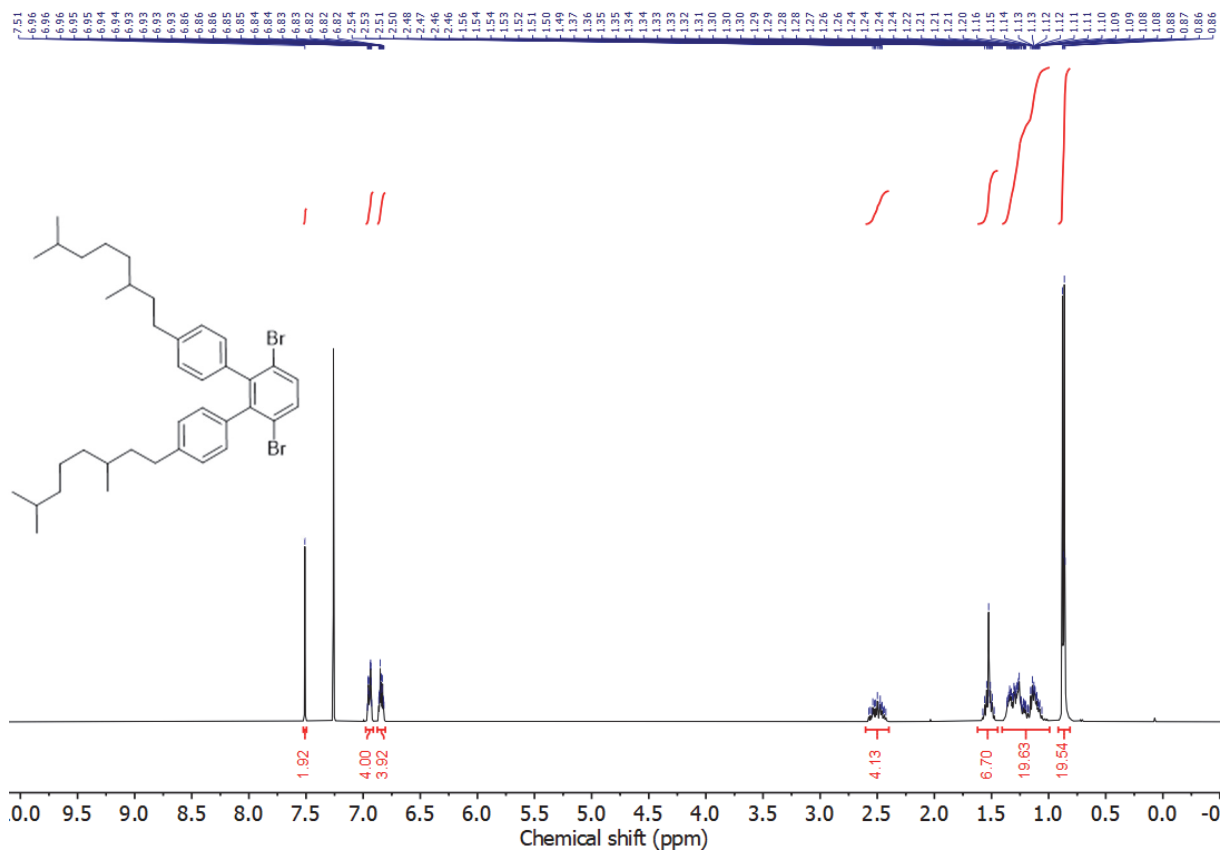
$^{13}\text{C}$  NMR spectrum of **3** ( $\text{CDCl}_3$ , 150 MHz,  $25^\circ\text{C}$ )



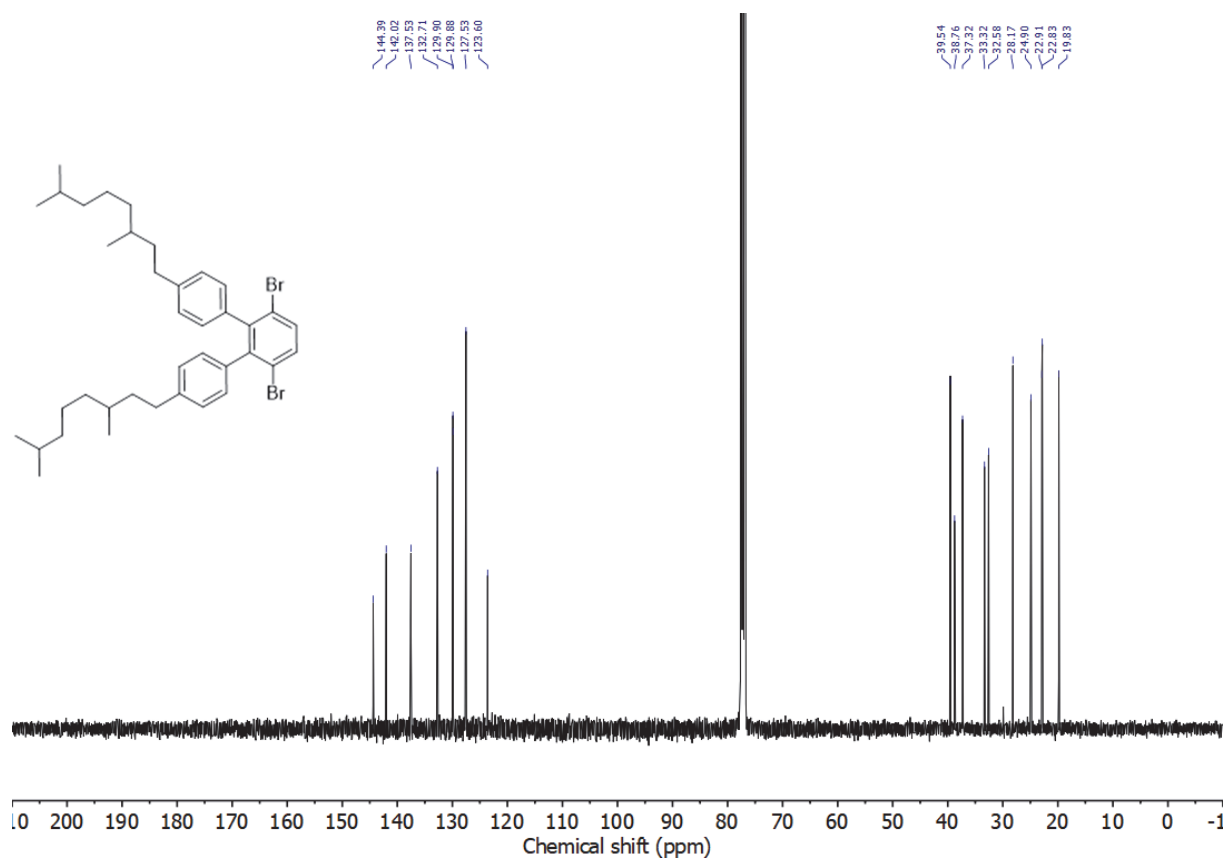
NMR spectrum of **4** ( $\text{CDCl}_3$ , 400 MHz,  $25^\circ\text{C}$ )



$^{13}\text{C}$  NMR spectrum of **4** ( $\text{CDCl}_3$ , 100 MHz,  $25^\circ\text{C}$ )

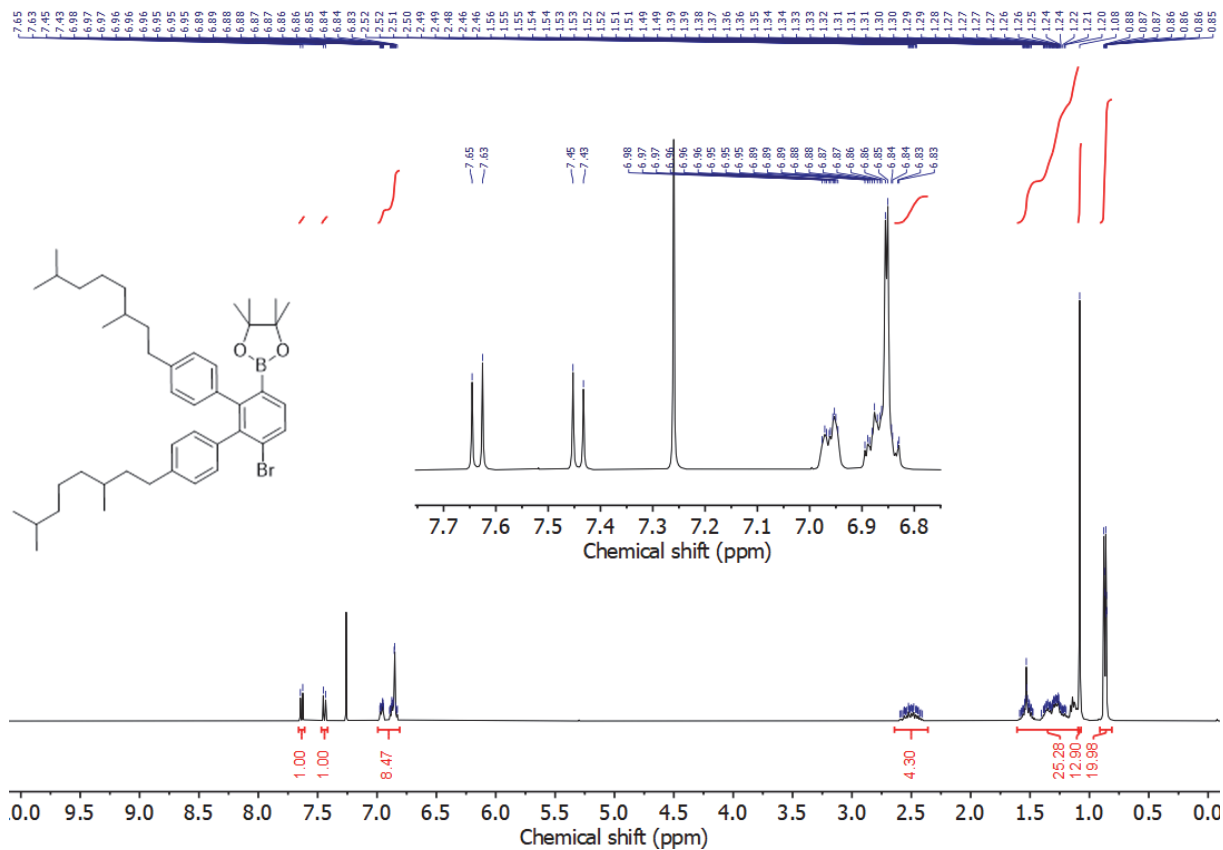


$^1\text{H}$  NMR spectrum of **5** ( $\text{CDCl}_3$ , 400 MHz,  $25^\circ\text{C}$ )

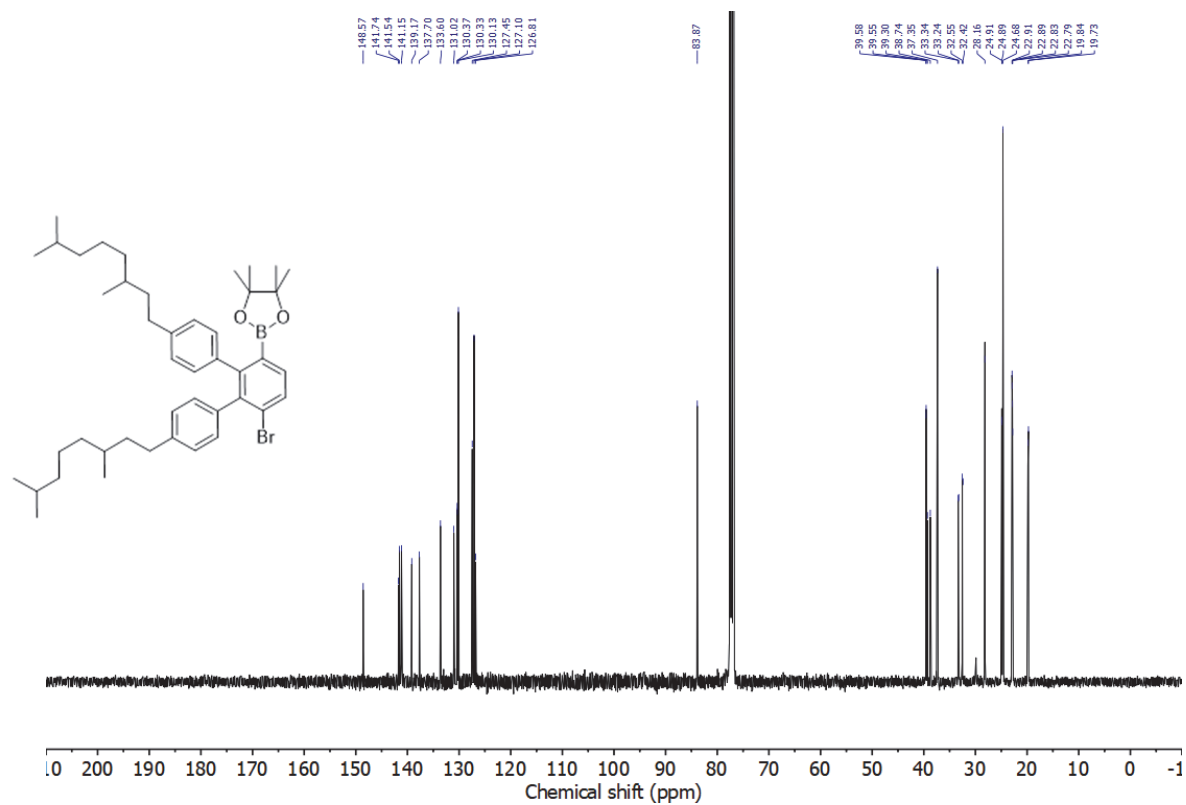


$^{13}\text{C}$  NMR spectrum of **5** ( $\text{CDCl}_3$ , 100 MHz,  $25^\circ\text{C}$ )





$^1\text{H}$  NMR spectrum of **6** (CDCl<sub>3</sub>, 400 MHz, 25°C)



$^{13}\text{C}$  NMR spectrum of **6** (CDCl<sub>3</sub>, 100 MHz, 25°C)

## Supporting Figures – Spectroscopic Characterization 9-aGNRs

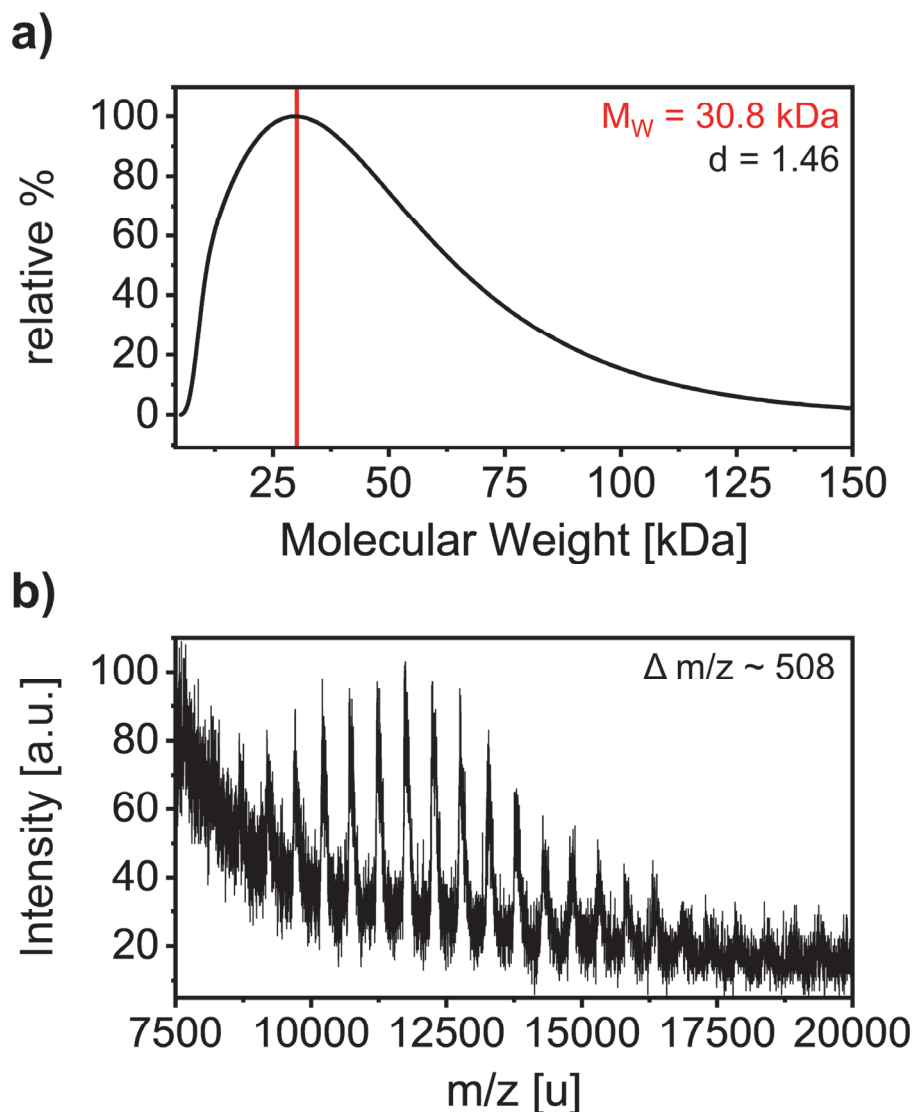


**Figure S1. Length Characterization of 9-aGNR precursor polymer.** **a)** Size exclusion chromatogram of a solution of precursor polymer in THF against a polystyrene standard. The determined  $M_w$  is marked by a red line in the chromatogram. The depicted  $M_w$  corresponds to 60 coupled terphenyl units and a length of  $\sim 25$  nm. **b)** MALDI-TOF mass spectrum of precursor polymer. Peaks are spaced by  $\sim 508$  u which corresponds to the molecular weight of a monomer unit. Peaks can be clearly observed up to a  $m/z$  ratio of 17500, indicating a length of  $\sim 35$  terphenyl units, corresponding to  $\sim 15$  nm.

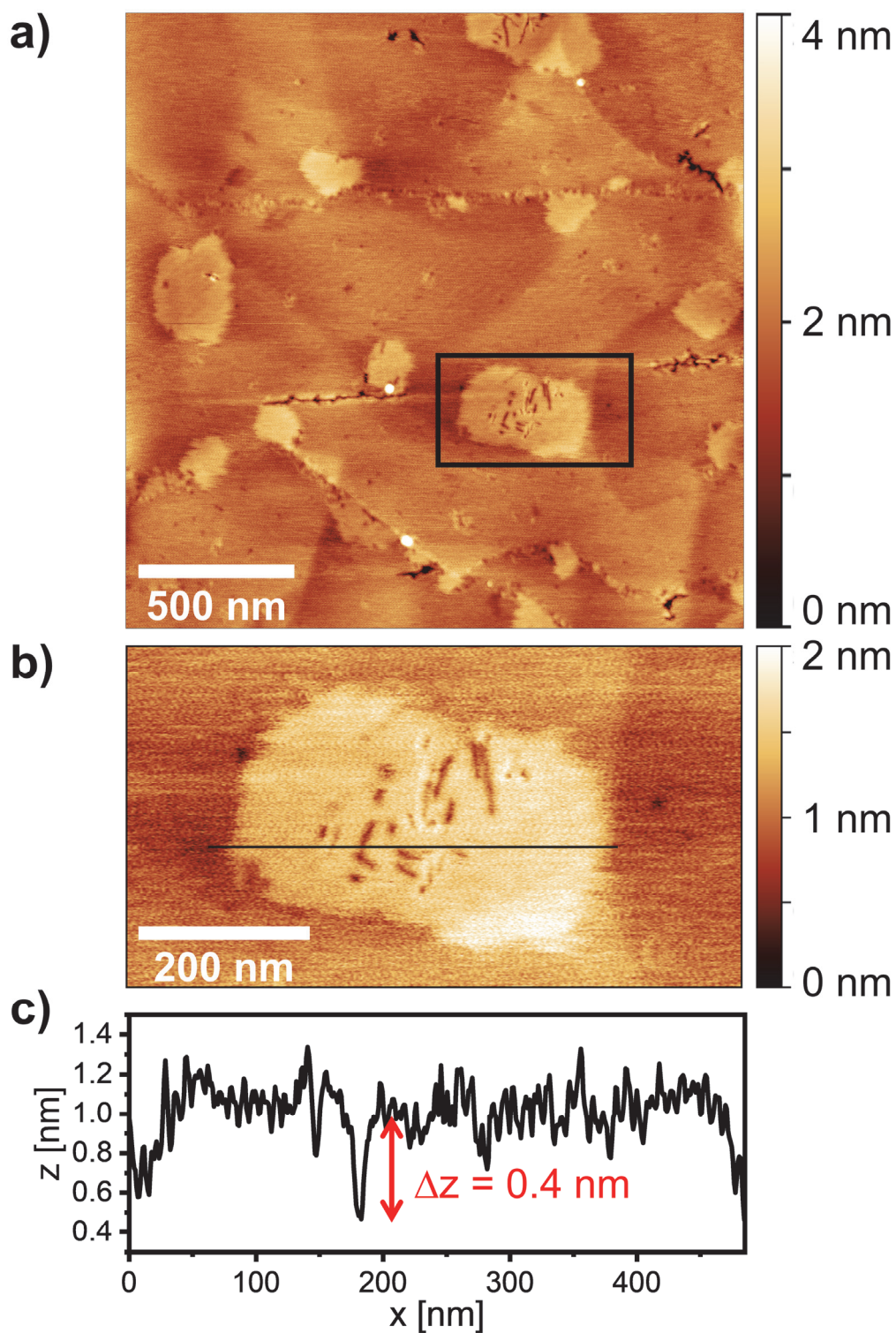


**Figure S2. a)** Tapping-mode AFM image (Bruker Dimension Icon equipped with OLTESPA-V3 tips) of self-assembled 9-aGNRs on freshly cleaved HOPG. 15  $\mu$ L of a diluted dispersion (optical density of 0.04 at 820 nm) of the 0.2-1 kg fraction 9-aGNR in toluene were drop-cast onto a freshly cleaved HOPG substrate. The substrate temperature was held at 50  $^{\circ}$ C for 5 minutes and then increased to 80  $^{\circ}$ C for another 10 min to facilitate slow evaporation of solvent. The image shows several small irregular islands that originate from GNR self-assembly

**b)** Zoom-in on the highlighted area in (a) showing an island of self-assembled GNRs. While individual GNRs cannot be resolved, ribbon-shaped vacancies in the island indicate the presence of GNRs with different lengths in the dispersion. **c)** Height profile along the line in (b) confirming the height of a nanoribbon island as 0.4 nm as previously reported by Li *et al.*<sup>1</sup>

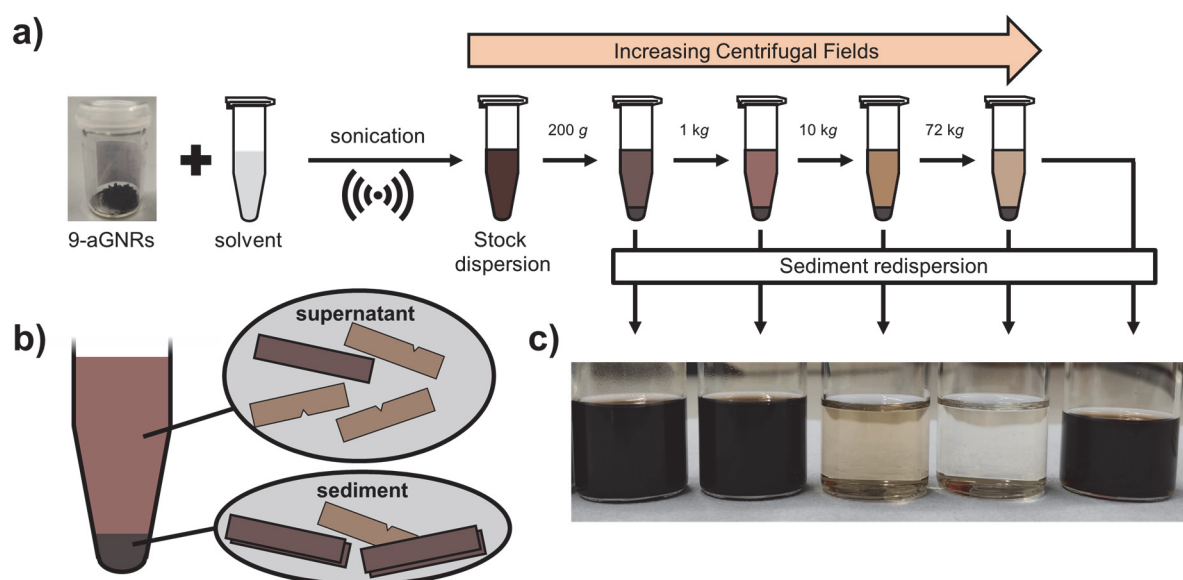


**Figure S3.** **a)** Schematic depiction of dispersion and liquid cascade centrifugation (LCC) process. 9-aGNRs are exfoliated in THF or toluene *via* sonication. The resulting stock dispersion is then centrifuged at 200 g. The supernatant is carefully removed and subjected to another centrifugation step at higher RCF, while the sediment is redispersed in fresh solvent. This process is repeated at RCF values of 1 kg, 10 kg and 72 kg. **b)** The sediment is expected to contain aggregated and mostly defect-free GNRs, while the supernatant should contain mostly defective GNRs. With each centrifugation step, more defect-free GNRs are removed from the dispersion. **c)** Photograph of the resulting dispersions.

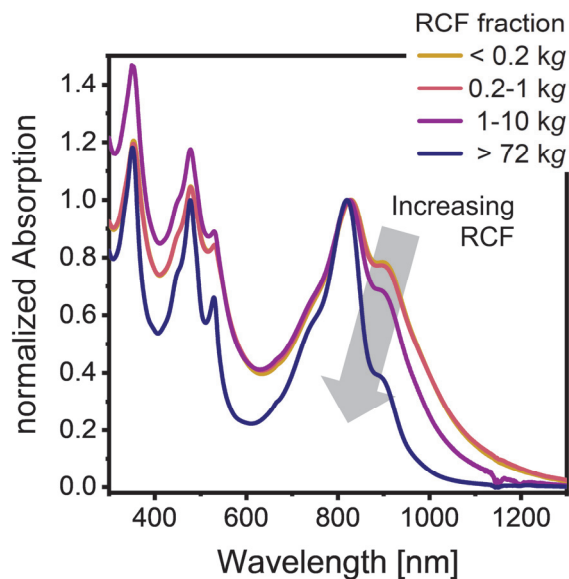


**Figure S4.** Absorption spectra for resulting 9-aGNR dispersions in toluene after LCC. A slight redshift of  $\sim 2$  nm of the peak maxima compared to dispersions in THF can be explained with the different dielectric environment of the two solvents.

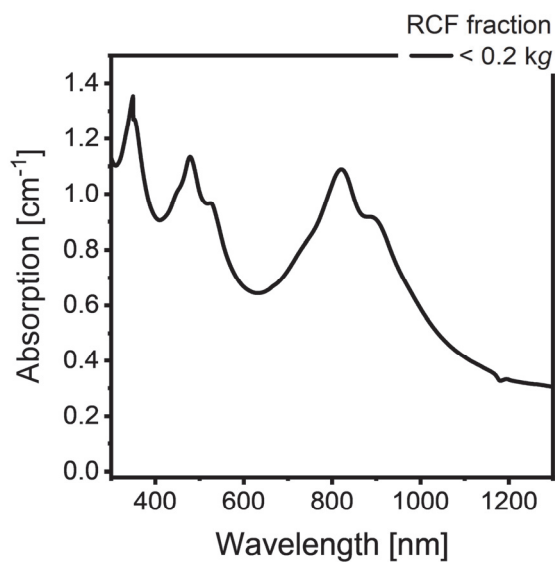


**Figure S5.** Uncorrected absorption spectrum for  $< 0.2$  kg fraction in THF. The spectrum shows a scattering background with an onset of  $\sim 0.3$  at 1300 nm.

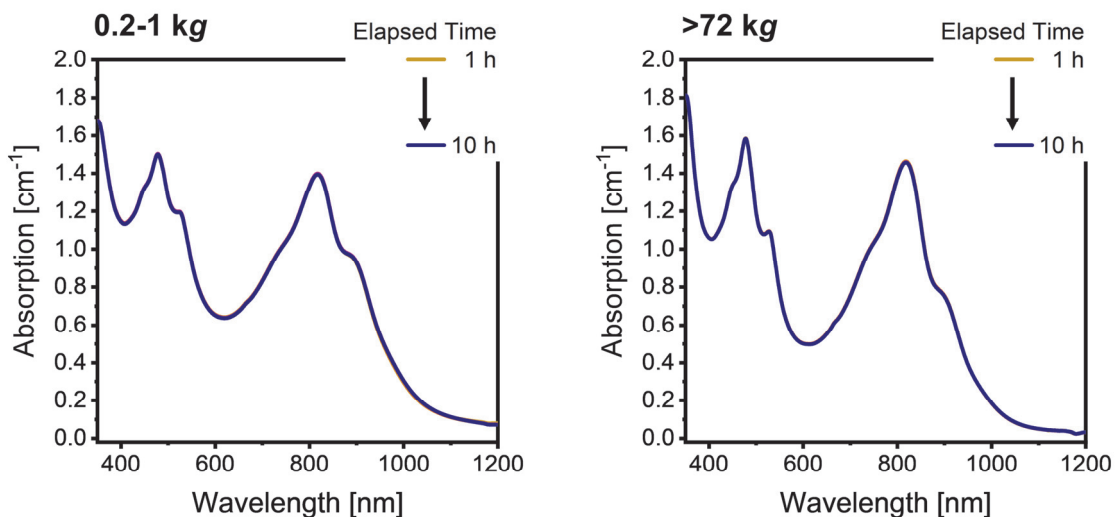


**Figure S6.** Absorption spectra of exfoliated 9-aGNRs in THF over 10 h. Spectra were measured once per hour for 10 h without moving the cuvette. As absorption spectra do not change, the first spectrum is barely visible. This indicates a high dispersion stability.

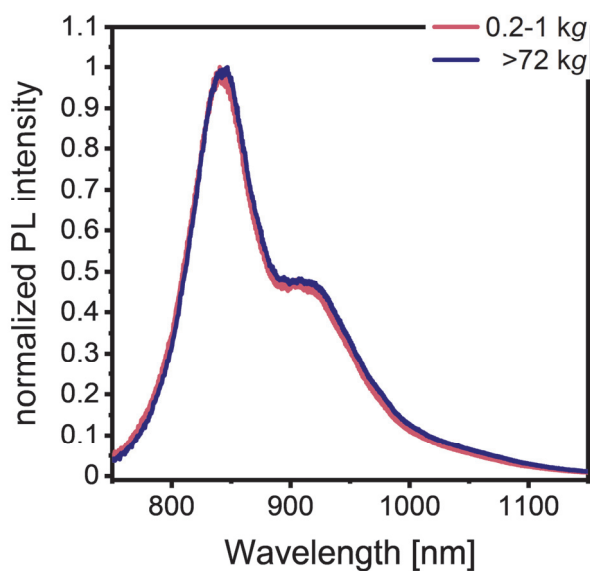


**Figure S7.** PL spectra of a 0.2-1 kg >72 kg 9-aGNR fraction in toluene.

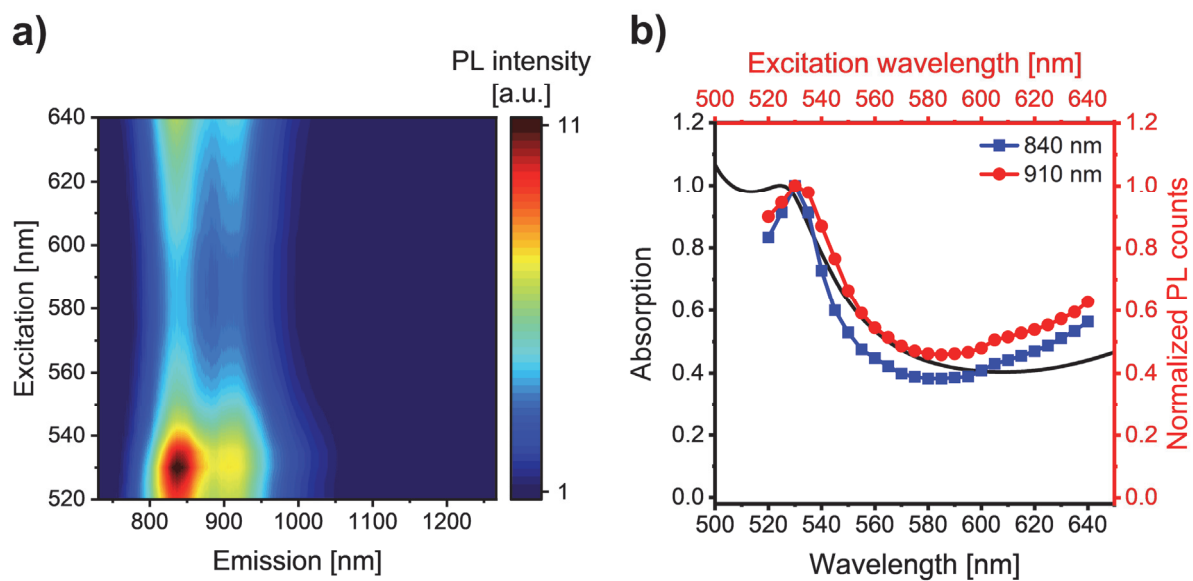


**Figure S8. a)** PL excitation-emission map of a >72 kg 9-aGNR fraction. **b)** Excitation spectrum obtained for emission at 840 nm (blue) and 920 nm (red). An absorption spectrum of the corresponding >72 kg fraction normalized to the absorption at 525 nm is shown as a black line for comparison.

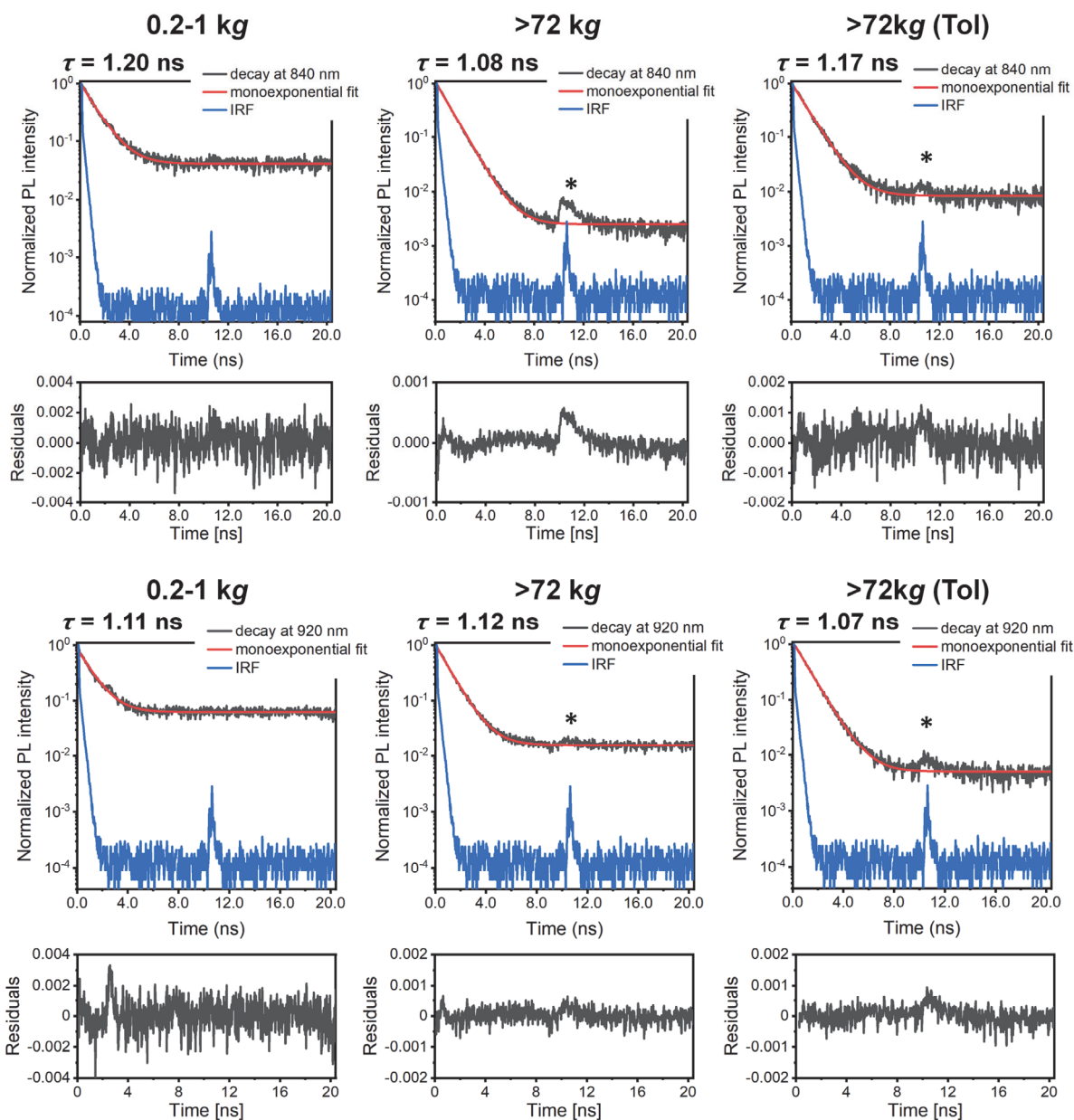


**Figure S9.** TCSPC histograms for PL decay at the emission features at 840 nm (upper panel) and 920 nm (lower panel) under excitation at 535 nm. The measured instrument response function (IRF) is shown in blue. Histograms were measured for 0.2-1 kg and >72 kg 9-aGNR fractions in THF and a >72 kg 9-aGNR fraction in toluene. The peak at 10 ns (marked with an asterisk) also appears in the IRF and is an artefact of the TCSPC setup. All histograms were fitted with a mono-exponential tail-fit procedure (fit function  $f(t) = A \cdot e^{-\frac{t-t_0}{\tau}} + c$ , where  $\tau$  is the extracted PL lifetime). Residuals of the fitting procedures are shown below. The extracted lifetimes vary between 1.0 and 1.2 ns with those at 920 nm being insignificantly shorter than those at 840 nm. Although fitting two exponential decays with different amplitudes should be possible for the expected two different GNR species, such multi-parameter fits would not be reliable for the available data.



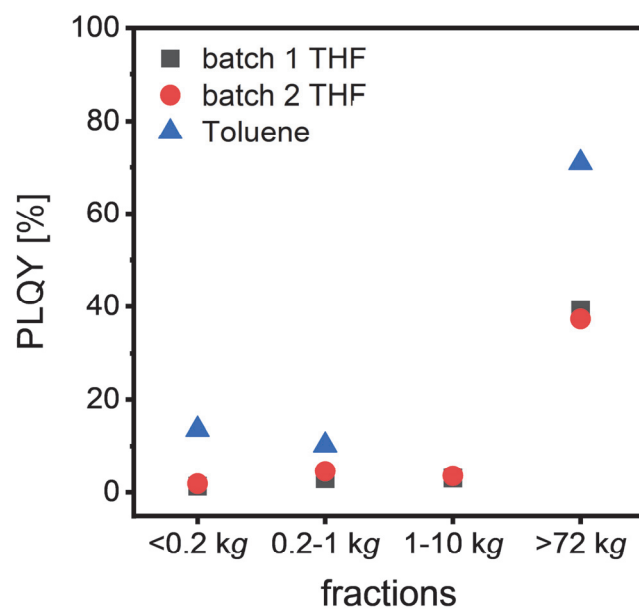


**Figure S10.** PL quantum yields (PLQY) of 9-aGNR dispersions in THF and toluene. PLQYs increase with increasing RCF.

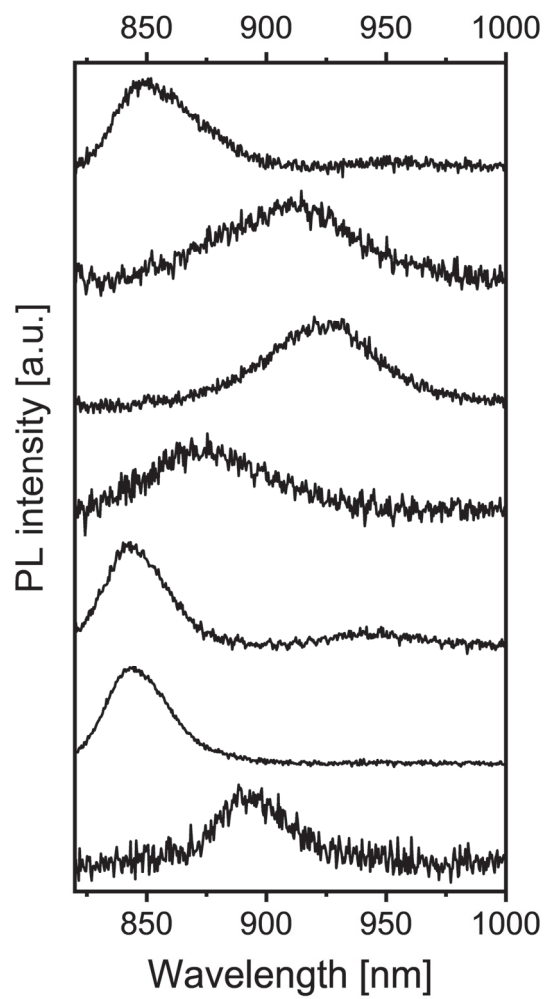


**Figure S11.** Room temperature PL spectra of 0.2-1 kg 9-aGNRs embedded in a polystyrene matrix.

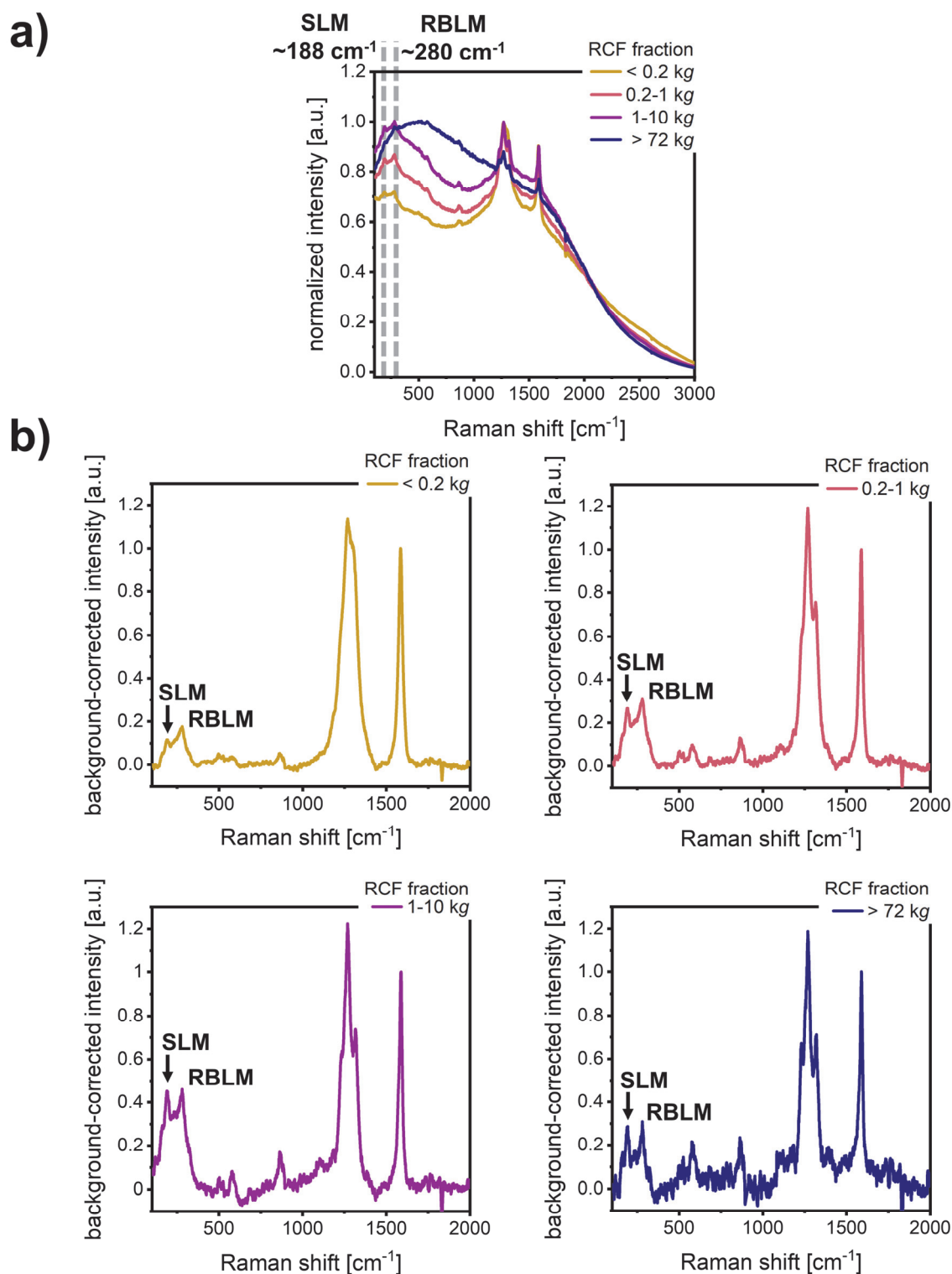


**Figure S12.** Raman spectra of exfoliated 9-aGNRs excited with a 785 nm laser. **a)** Uncorrected Raman spectra showing a high PL background. The RBLM at  $280\text{ cm}^{-1}$  and SLM at  $188\text{ cm}^{-1}$  (dashed lines) are clearly visible in all LCC fractions. **b)** Background-corrected Raman spectra for all fractions.

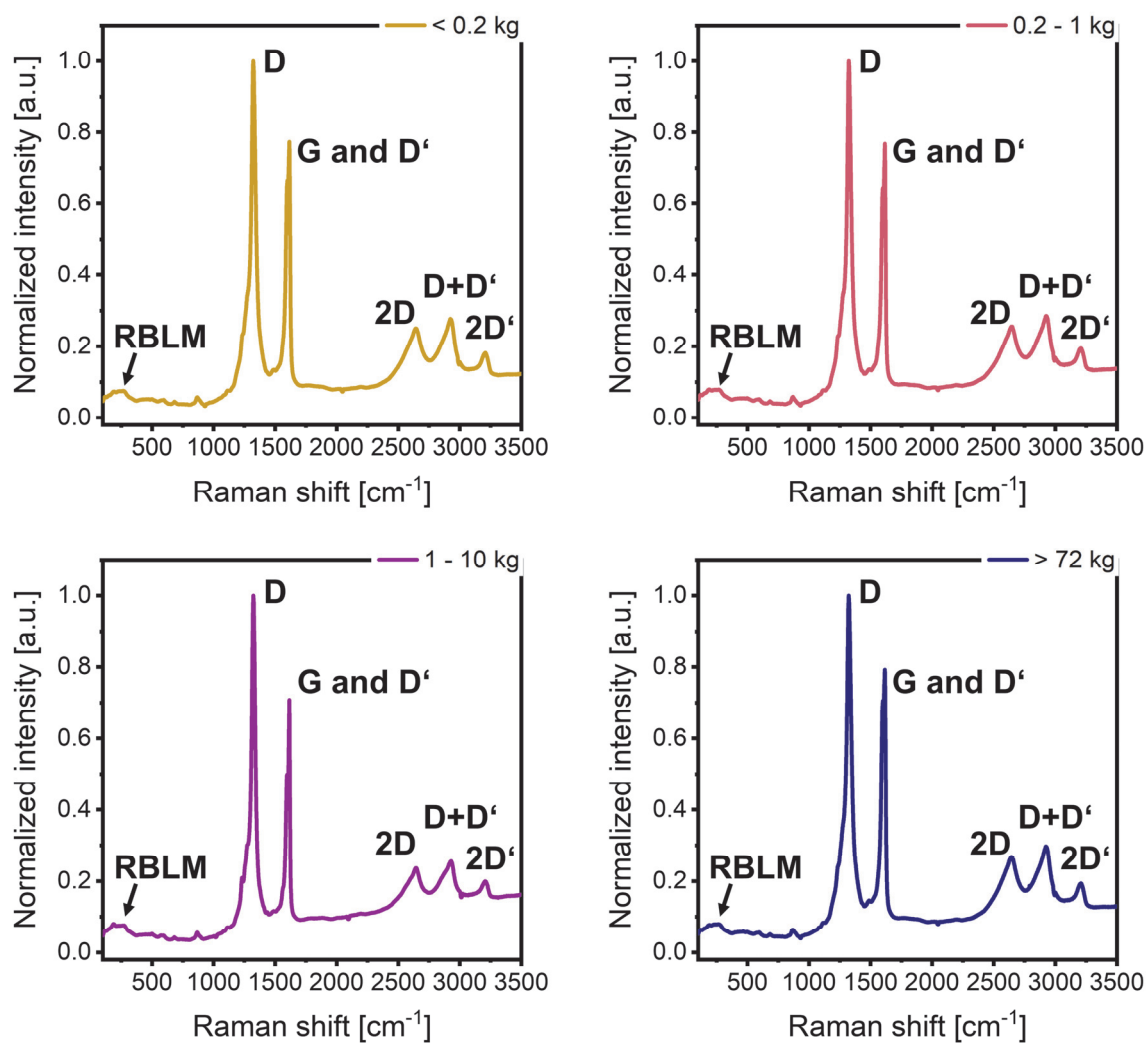


**Figure S13.** Full range Raman spectra of all LCC fraction of exfoliated 9-aGNRs in THF (as shown in Figure 4 of the main text) excited with a 532 nm laser.

## Quantum chemical calculations of neutral 9-aGNRs

All optimized geometries are available at the following data repository:

<https://doi.org/10.11588/data/JAV0ZK>

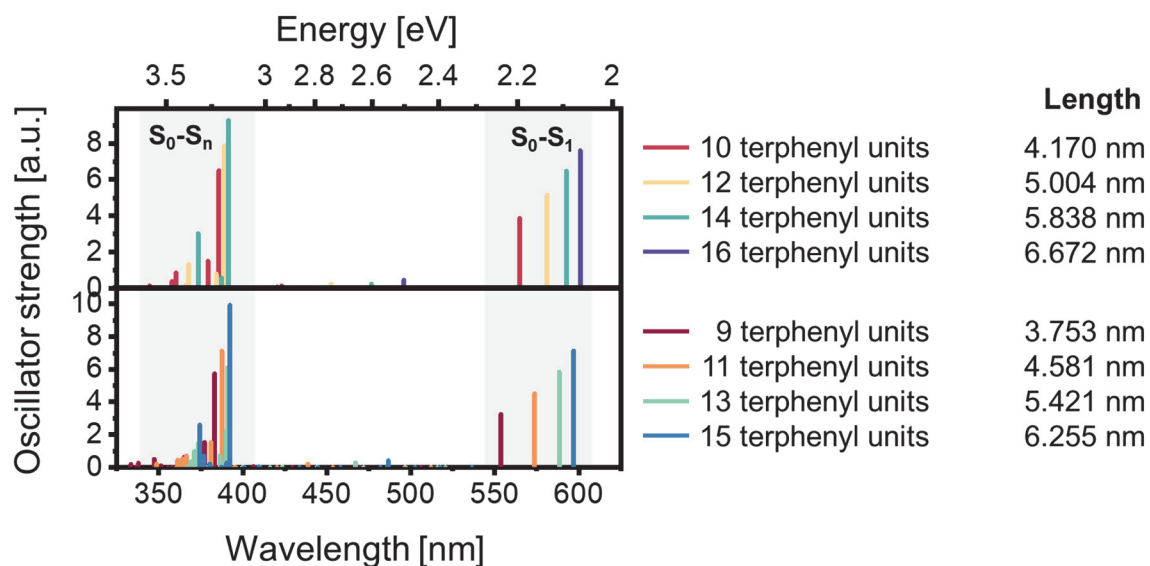
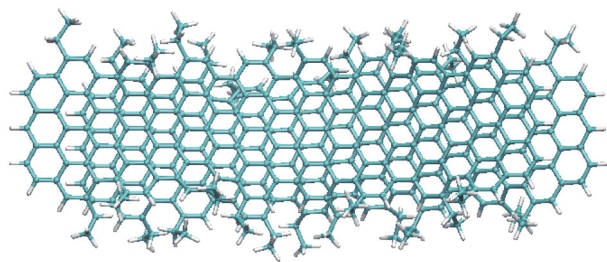


**Figure S14:** Comparison between the excited state vertical transition energies as computed at the TD-DFT ( $\omega$ B97X-D/6-31G\*) level for different oligomers with parallel (top) and trapezoidal (bottom) shapes.

**Top view**



**Side view**

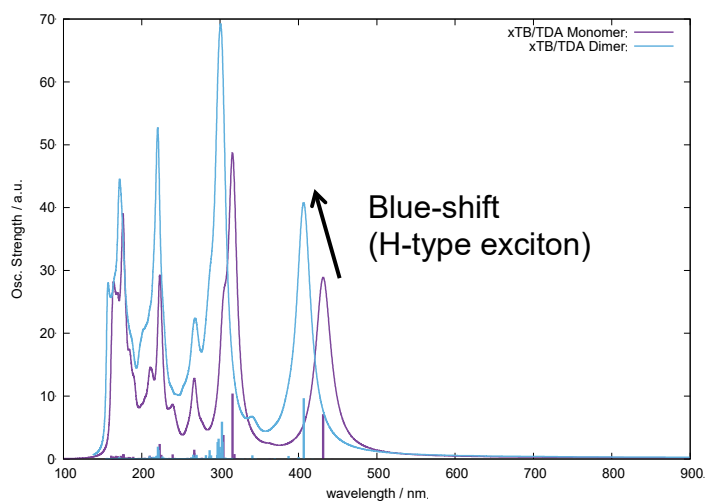
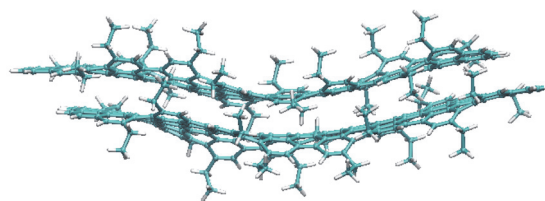


**Figure S15.** GFN2-xTB optimized geometry for the 9-aGNR dimer (top and side views). Comparison between the sTD-DFT transition energies (unscaled values) computed for the monomer (purple line) and dimer (light blue line).

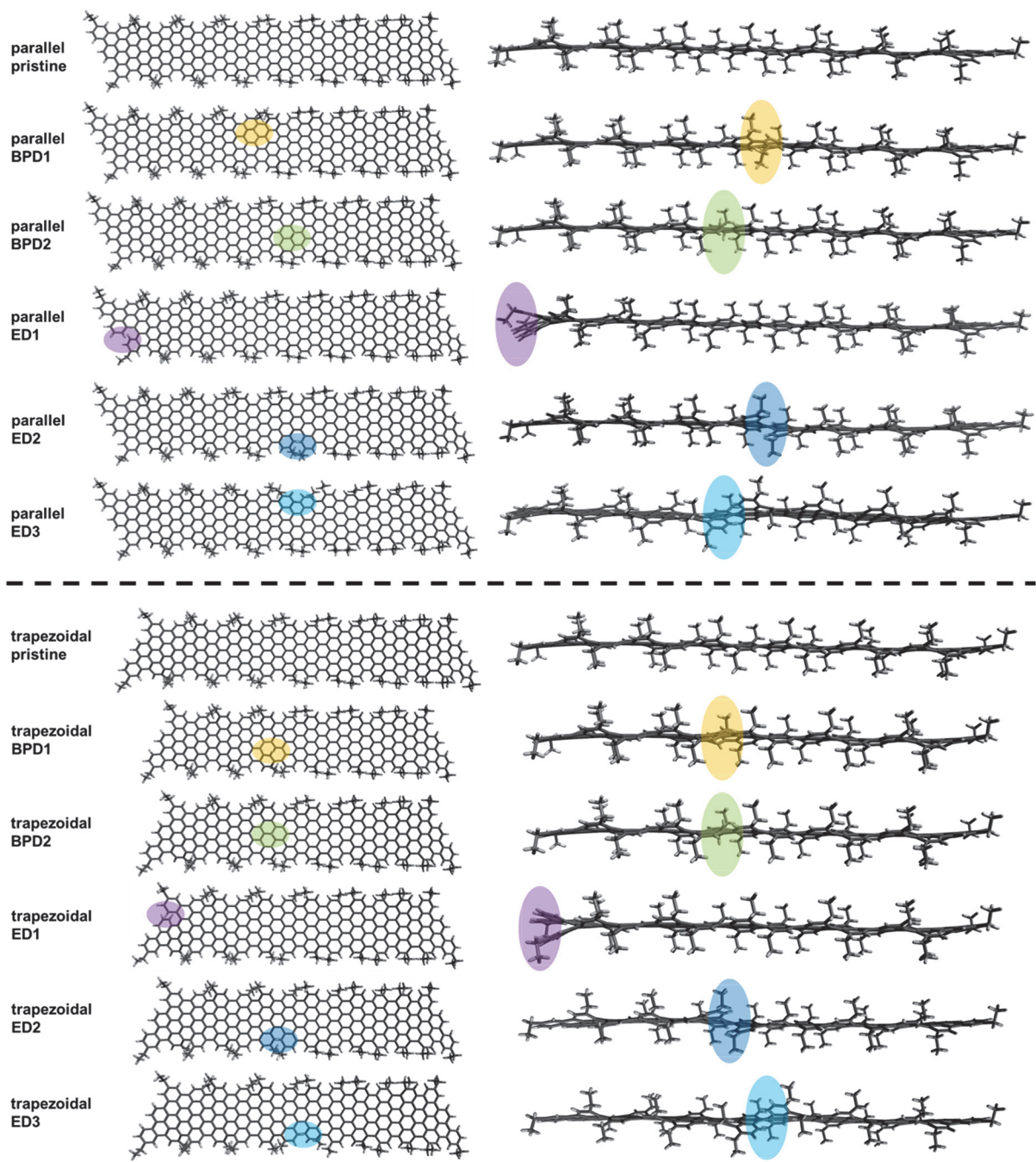


**Figure S16.** Optimized (GFN2-xTB) structures for parallel 9-aGNRs (top panel) and trapezoidal 9-aGNRs (bottom panel). The coloured regions highlight the positions of the respective defect.

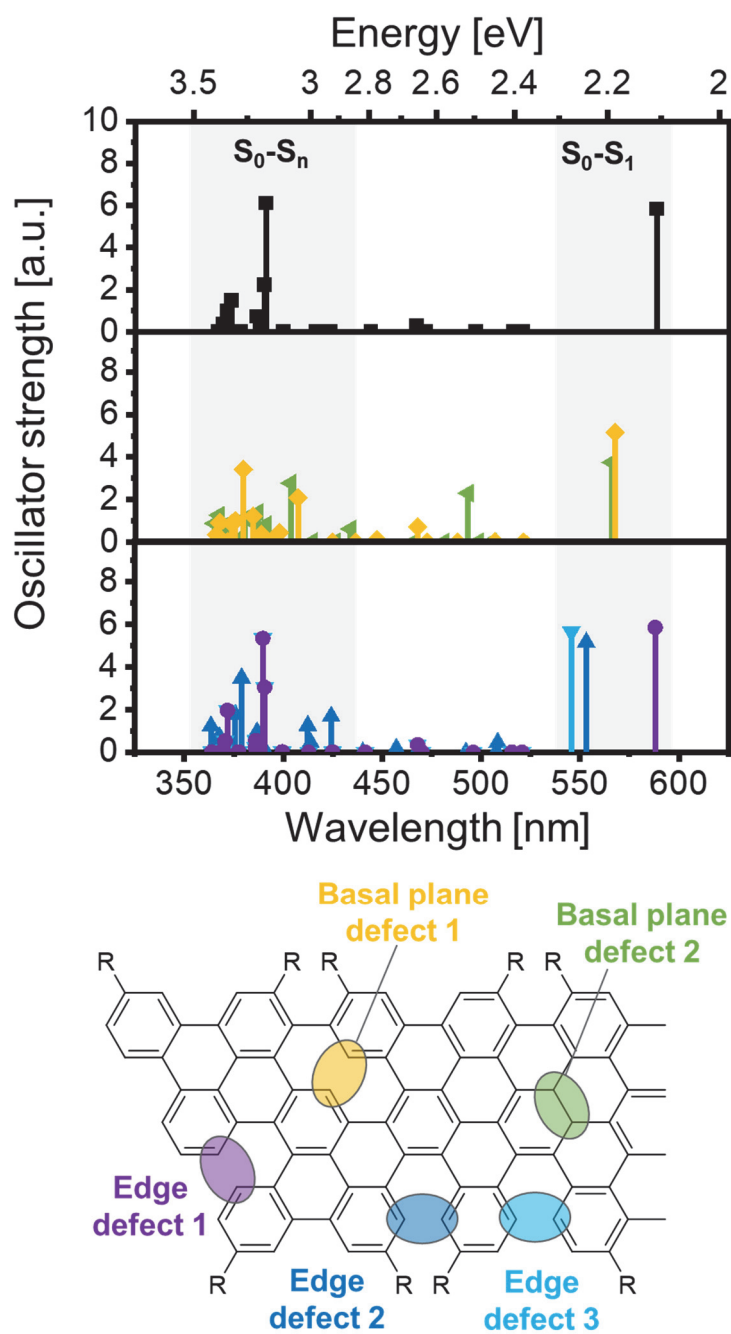


**Figure S17:** TD-DFT transition energies computed for the **trapezoidal 9-aGNR**: comparison between pristine and defected nanoribbons. Pristine (top panel, black line), BP1 (middle panel, yellow line), BP2 (middle panel, green line), ED1 (bottom panel, purple line), ED2 (bottom panel, dark blue line), ED1 (bottom panel, light blue line).



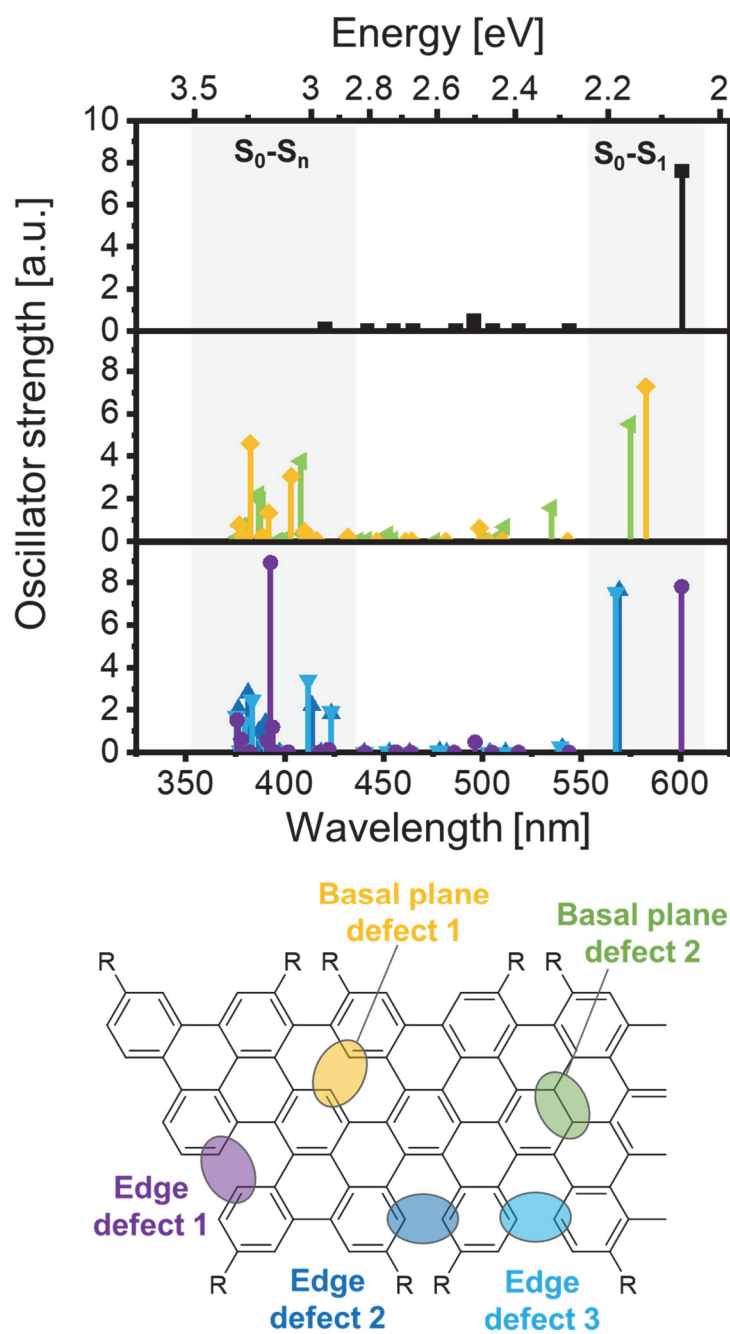


**Figure S18:** TD-DFT transition energies computed for the **parallel 9-aGNR**: comparison between pristine and defected nanoribbons. Pristine (top panel, black line), BP1 (middle panel, yellow line), BP2 (middle panel, green line), ED1 (bottom panel, purple line), ED2 (bottom panel, dark blue line), ED1 (bottom panel, light blue line).

## Supporting Figures – Doped 9-aGNRs

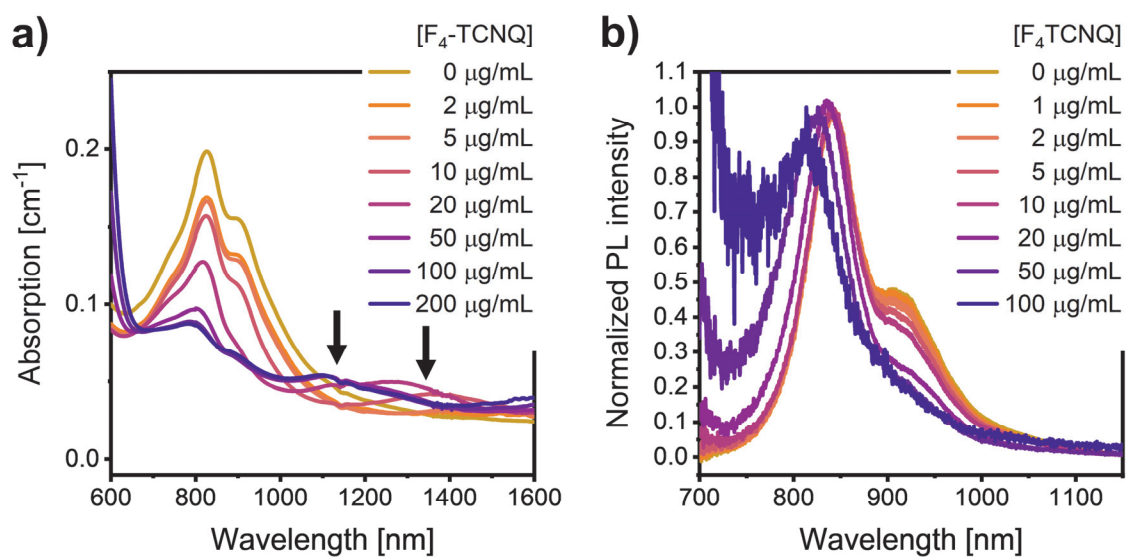


**Figure S19.** a) Absorption spectra of a >0.2-1 kg 9-aGNR dispersion doped with F<sub>4</sub>TCNQ. Charge-induced absorption peaks are marked by arrows. b) Normalized PL spectra of a >0.2-1 kg 9-aGNR dispersion doped with F<sub>4</sub>TCNQ showing blue-shift and concentration-dependent quenching of the main emission peaks.

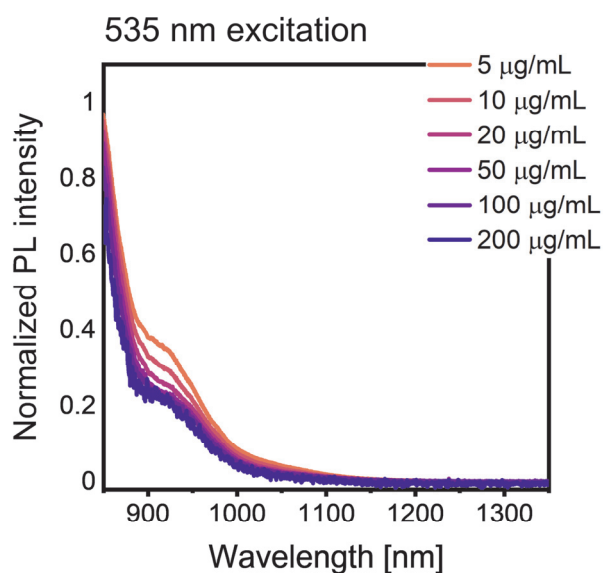


**Figure S20.** PL spectra of F<sub>4</sub>TCNQ-doped >72 kg 9-aGNR dispersions recorded at longer wavelengths. No new red-shifted emission features are visible.

## Quantum chemical calculations of charged 9-aGNRs

The structure of doped (i.e., positively charged species, +1) 9-aGNRs was optimized at the GFN2-xTB level. The electronic transitions were computed at the TD-UDFT level (U $\omega$ B97X-D/6-31G\*).

The calculated electronic transitions of undoped - neutral (yellow bars) vs. doped - charged (purple bars) 9-aGNR of trapezoid (upper panel) and parallel (bottom panel) shapes are compared in **Figure S21**. For each species (in their neutral and charged state) we considered the pristine case (without defects) and the presence of an edge defect type 2 (ED2). Charged species show dipole allowed electronic transitions lower in energy than the neutral species (see 700-1000 nm region). The shapes (trapezoid or parallel) and the structural defects, slightly affect the transition energies of charged species.

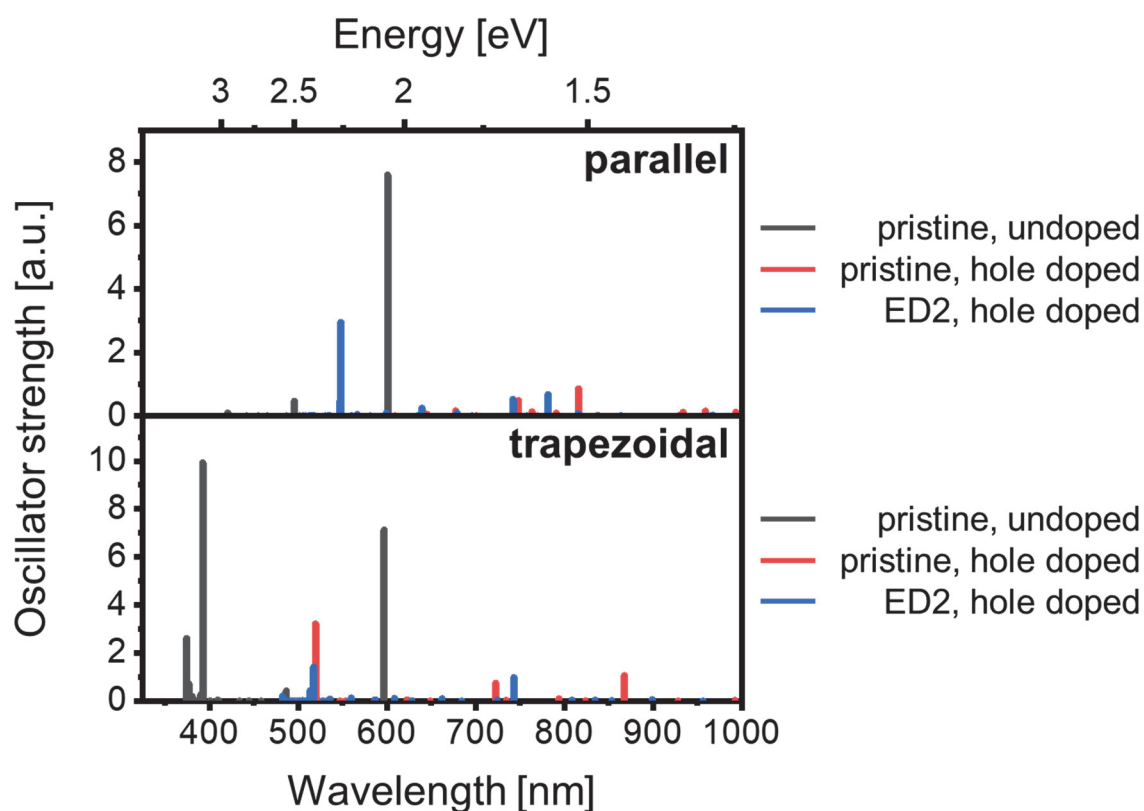


**Figure S21:** Comparison between the TD-UDFT (U $\omega$ B97X-D/6-31G\*) transition energies (unscaled data) computed for the parallel (top) and trapezoidal (bottom) 9-aGNRs for their pristine undoped (neutral, black line), pristine doped (charged, +1, red line) and defective ED2 doped species (charged, +1, blue line). The structural models considered refer to 16 terphenyl units for the parallel shape, and 15 units for the trapezoidal shape.

## REFERENCES

1. Li, G.; Yoon, K. Y.; Zhong, X.; Zhu, X.; Dong, G., Efficient Bottom-Up Preparation of Graphene Nanoribbons by Mild Suzuki-Miyaura Polymerization of Simple Triaryl Monomers. *Chemistry* **2016**, *22* (27), 9116-20.